Geochemical Properties and Saline-Water Intrusion in the Valle de Yabucoa Alluvial Aquifer, Southeastern Puerto Rico

By Joseph W. Troester and Ronald T. Richards

U.S. DEPARTMENT OF THE INTERIOR
BRUCE BABBITT, Secretary

U.S. GEOLOGICAL SURVEY
Gordon P. Eaton, Director

CONTENTS

FIGURES

TABLES

CONVERSION FACTORS AND ABBREVIATED UNITS

Multiply	By	To obtain
kilometer (km)	0.62137	mile
meter (m)	3.2808	feet
centimeter (cm)	0.3937	inch
millimeter (mm)	0.03937	inch
micrometer (μm)	0.00003937	inch
square kilometer (km^2)	0.3861	square mile
cubic meters per second (m^3/s)	35.31467	cubic feet per second
cubic meters per second (m^3/s)	15,850	gallons per minute
Liters per second (L/s)	15.85032	gallons per minute
cubic meters per day per meter of drawdown [(m^3/d)/m]	0.05992	gallons per minute per foot of drawdown

Temperature: In this report temperatures are given in degrees Celsius (°C).

Temperatures may be converted to degrees Fahrenheit (°F) as follows:

$$F = (9/5 \times °C) + 32$$

Abbreviated water-quality, concentration, and geophysical units used in this report:

micrograms per liter (μg/L)

micrograms per gram (μg/g)

milligram per liter (mg/L)

microsiemens per centimeter at 25 °C (μS/cm)

millisiemens per meter (mS/m)

Microsiemens per centimeter can be converted to millisiemens per meter as follows:

10 μS/cm = 1 mS/m

Ohm-meters can be converted to millisiemens per meter as follows:

Ω-m = 1,000/(mS/m)

Geochemical Properties and Saline-Water Intrusion in the Valle de Yabucoa Alluvial Aquifer, Southeastern Puerto Rico

By Joseph W. Troester and Ronald T. Richards

ABSTRACT

The Valle de Yabucoa alluvial aquifer is located along the southeastern coast of Puerto Rico and is the municipal and industrial water supply for the town of Yabucoa. The aquifer consists of more than 100 meters of alluvium overlying relatively impermeable bedrock. Water in the aquifer has iron and manganese concentrations as high as 28 and 3.6 milligrams per liter, respectively. Although the elevated iron and manganese concentrations in the aquifer pose no health threat, they frequently exceed the secondary standards for drinking water established by the U.S. Environmental Protection Agency of 0.3 milligrams per liter for iron and 0.05 milligrams per liter for manganese. Pumping from the aquifer for industrial use and public supply has lowered the water table to below sea level in some areas and has reversed the natural gradient of the water table toward the ocean. The saline-freshwater interface appears to have migrated landward because of this gradient reversal. A subsequent reduction in the rate of pumping has caused the water table to rise and may have stopped the landward migration of saline water. Two surface electromagnetic geophysical techniques (the terrain conductivity method and the transient electromagnetic method) were used to map depth to bedrock and the position of the saline-freshwater interface. Pumping and the shape of the bedrock-alluvium contact appear to control the extent and location of the saline-freshwater interface. The data indicate that saline-water intrusion probably is confined to the lowest part of the aquifer in a narrow paleochannel incised in the bedrock.

INTRODUCTION

The principal economic activities within the Valle de Yabucoa in southeastern Puerto Rico are related to agriculture (sugarcane, pasture, and plantains) and manufacturing (by an oil refinery, a cigarette manufacturing plant, and a sugar mill). The alluvial aquifer, which underlies the 45-km^2 valley floor, supplies nearly all of the water used for domestic, commercial, and industrial purposes. Locally, ground-water quality can be considered unsuitable for some uses because of the presence of high concentrations of dissolved iron and manganese. Elevated concentrations of these elements probably do not pose a human health threat, but both have a low taste threshold, contribute to water hardness, and readily stain kitchen and bathroom fixtures and laundry (Viessman and Hammer, 1985). The U.S. Environmental Protection Agency secondary standards for drinking water are 0.3 mg/L for iron and 0.05 mg/L for manganese (U.S. House of Representatives, 1996). In 1989, the U.S. Geological Survey (USGS), in cooperation with the Puerto Rico Aqueduct and Sewer Authority (PRASA) began an investigation to determine the sources of iron and manganese and the mechanisms controlling their distribution in the ground water in the Valle de Yabucoa alluvial aquifer.

In July 1990, water levels were measured in wells throughout the valley and a water-level cone of depression was detected near the coast (Collar and others, 1990). At that time, withdrawal of ground water for industrial use and for public supply had lowered water levels in the center of this cone of depression to 12 m below mean sea level and caused the potentiometric surface to slope from the ocean to the pumping center, 2 km from the coast.

Because some wells had already been adversely affected by the saline intrusion, the U.S Geological Survey entered into additional cooperative agreements with the Puerto Rico Industrial Development Company (PRIDCO) in 1992 and PRASA in 1994 to address this threat of saline-water intrusion to the public and industrial water supply. The on-going investigation of elevated iron and manganese concentrations in the ground water was expanded to locate and define the saline-freshwater interface and the controls, including the depth to bedrock, on saline intrusion in the Valle de Yabucoa alluvial aquifer.

Purpose and Scope

This report summarizes the results of a study to describe the hydrogeology and geochemistry of the Valle de Yabucoa alluvial aquifer and to define the occurrence and potential for saline-water intrusion in the aquifer, which includes mapping the depth to bedrock in the lower part of the valley. The study was conducted in the Valle de Yabucoa in southeastern Puerto Rico (fig. 1). The scope of the investigation included the collection and evaluation of water-quality, ground-water, and surface-water data. Water-quality samples were collected from 44 wells. In July of 1990, stream-discharge and water-level data were collected from a number of streams and wells throughout the valley to define the extent of the cone of depression in the water table potentiometric surface.

A surface geophysical survey of the valley using two electromagnetic techniques (the terrain conductivity method and the transient electromagnetic method) was undertaken to define the depth to bedrock and the location of the saline-freshwater interface.

Collection of geophysical field data began in December of 1990 and continued until June 1991. Several observation wells were drilled throughout the valley to determine water quality and the change in hydraulic head in the aquifer with depth. The data from the geophysical surveys were used to determine the best location for the deepest and last observation well. That observation well was constructed between November 1992 and February 1993 and water-level and water specific conductance data were collected from February 1993 until November 1995. This well will continue to be useful for monitoring the intrusion of saline water into the Valle de Yabucoa.

Acknowledgments

GEOLOGY, CLIMATE, AND GEOMORPHOLOGY OF THE VALLE DE YABUCOA

The Valle de Yabucoa is a 45 km^2 alluvial valley along the southeastern coast of Puerto Rico (fig. 1). The valley is surrounded by the hills of the San Lorenzo Batholith on three sides and by the Caribbean Sea on the fourth. The study area has a tropical marine climate and receives an average annual precipitation of about 2,046 mm. The intense precipitation is drained by the Río Guayanés, Caño de Santiago, the Río del Ingenio, and minor tributaries.
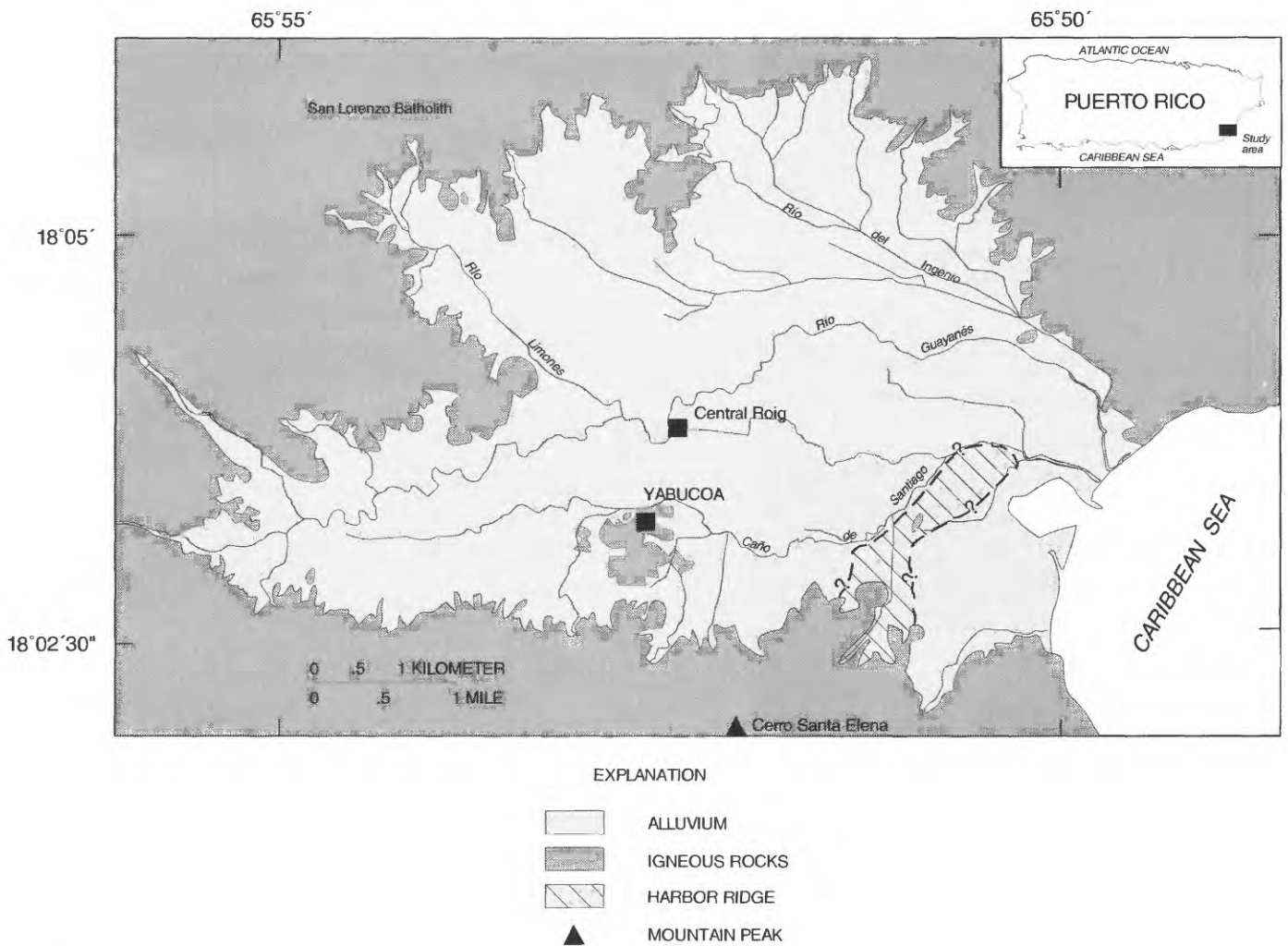
Figure 1. Location of the Valle de Yabucoa, Puerto Rico, the boundary of the alluvial valley fill, major streams, and cultural features.

Geology

The early work on the geology of southeastern Puerto Rico was conducted by Lobeck (1922), Fettke (1924a, b), and Meyerhoff (1933). More recently, general geologic maps of Puerto Rico have been produced by Briggs and Akers (1965) and Cox and Briggs (1973). Detailed geologic maps of the study area were produced by Rogers (1977) and Rogers and others (1979).

San Lorenzo Batholith

The hills surrounding the Valle de Yabucoa are composed of the San Lorenzo Batholith, a large, igneous intrusive body. These plutonic rocks were first described by Fettke (1924a). According to Rogers (1977), the San Lorenzo Batholith is a composite body that occupies an area of about 500 km^2 in southeastern Puerto Rico and is composed of gabbro, diorite, tonalite, granodiorite, and quartz monzonite. Rogers and others (1979) divided the batholith into three major units, which from oldest to youngest include a diorite and gabbro unit, the granodiorite of San Lorenzo (and associated tonalite facies), and the plutonic complex of Punta Guayanés. The batholith also contains a few roof pendants of metavolcanic rock. Potassium-argon ages of the rocks (Cox and others, 1977; Rogers, 1977) indicate that the rocks were emplaced over a period of at least 12 million years during the Late Cretaceous and possibly the Early Paleocene.

The oldest unit, which is composed of diorite and gabbro, is exposed in the southwestern part of the Punta Guayanés quadrangle, south of the Valle de Yabucoa. This unit is intruded by both the San Lorenzo and Punta Guayanés rock units. According to Rogers (1977) the average composition of the rock, based on 17 modal analyses, is about 58 percent plagioclase, 3.5 percent quartz, 32 percent hornblende, 2.5 percent augite, 3.5 percent magnetite, 0.5 percent sphene, and minor orthoclase, apatite, and zircon. The plagioclase is andesine, ranges locally to sodic labradorite, and is generally partially altered to sericite and clay minerals.

The granodiorite and associated tonalite of the San Lorenzo unit were named by Rogers (1977) after the town of San Lorenzo, which is to the northwest of the Valle de Yabucoa. The granodiorite is part of a pluton that comprises at least 75 percent of the San Lorenzo Batholith. The rocks are exposed in a part of the northern Punta Guayanés quadrangle and in most of the Yabucoa quadrangle. The tonalite facies is exposed in the southwestern part of the Punta Guayanés quadrangle. Based on the outcrop pattern, Rogers (1977) suggests that the tonalite underlies most of the alluvium in the Valle de Yabucoa. The rocks of granodiorite and tonalite of the San Lorenzo unit are intruded by the plutonic complex of the Punta Guayanés unit. According to Rogers (1977) the average composition of the granodiorite, based on 16 modal analyses, is about 49 percent plagioclase, 12 percent orthoclase (20 percent of the total feldspar), 17 percent quartz, 17 percent hornblende, 2.5 percent biotite, 1.5 percent magnetite, 0.5 percent sphene, and minor augite, apatite, and zircon (percentages do not add to 100 because of rounding). The plagioclase is largely andesine but locally ranges from andesine to calcic oligoclase. The average composition of the tonalite, based on 17 modal analyses, is about 56 percent plagioclase, 4 percent orthoclase (7 percent of total feldspar), 23 percent quartz, 10 percent hornblende, 4 percent biotite, 1 percent magnetite, and minor augite, sphene, apatite, and zircon (percentages do not add to 100 because of rounding). Mineralogically, the tonalite closely resembles the granodiorite of San Lorenzo.

The youngest major unit within the San Lorenzo Batholith consists of many smaller plutons that range from quartz monzonite and granodiorite near the center of the batholith to tonalite near the margin. Rogers (1977) informally named the complex after Punta Guayanés. The rocks are exposed in the northern part of the Punta Guayanés quadrangle, to the north of the Valle de Yabucoa. According to Rogers (1977) the average composition of the main pluton of the Punta Guayanés complex, based on 20 modal analyses, is about 51 percent plagioclase, 13 percent orthoclase (20 percent of total feldspar), 32 percent quartz, 4 percent mafic minerals (biotite and very subordinate hornblende), 0.5 percent magnetite, and minor accessory sphene, apatite, and zircon (percentages do not add to 100 because of rounding). Plagioclase is largely oligoclase but ranges to sodic andesine.

The San Lorenzo Batholith in the study area contains no known mines or prospects. According to Rogers (1977) and Rogers and others (1979), rare traces of copper mineralization occur in all the major plutonic units and generally include chalcopyrite, malachite, and azurite. Rogers (1977) reports that a semi-quantitative spectrographic analysis of a mineralized nodule showed 2 percent copper, 0.3 percent manganese, more than 10 percent iron, and 0.3 percent titanium. Rogers and others (1979) report a small but rich mineralized zone found about 1.2 km west-northwest of Maunabo, just south of the study area. A semi-quantitative spectrographic analysis of a composite sample measured a content of more than 10 percent of both copper and iron, 0.2 percent titanium, 700 mg/kg vanadium, and 300 mg/kg manganese.

To the north of the study area, in the Humacao quadrangle, appreciable quantities of magnetite have been observed in a diorite-hornblendite complex that is part of the San Lorenzo Batholith (Cox and Briggs, 1973; M'Gonigle, 1978). Colony and Meyerhoff (1935) and Cadilla (1963) discuss this titaniferous iron ore prospect and the abandoned exploratory tunnels in detail. Colony and Meyerhoff (1935) report four partial chemical analyses of the ore with Fe_2O_3 concentrations ranging from 12.66 to 78.83 percent and TiO_2 concentrations ranging from 0.93 to 5.35 percent.

Alluvium

More than 100 m of alluvium overlie the San Lorenzo Batholith in the Valle de Yabucoa. The alluvium was derived from the erosion of the batholith. Mineral grains and rock fragments were transported and then deposited by the streams in the valley. The alluvium is composed of sand, silt, and clay with occasional pebbles, cobbles, and boulders and minor amounts of calcareous shell fragments and organic material. Most of the sand is yellowish-brown to medium-gray in color and intimately mixed with the yellowish-brown to grayish-green silt and clay. The sand is coarser and the sand beds are thicker and more common with increasing distance inland from the coast. However, there are large local variations in aggregate sand thickness and character. Beach and swamp deposits are present close to the coast. The mineralogy and chemistry of the alluvium and beach deposits have been studied by Guillou and Glass (1957), Collar and others (1990), Troester and others (1990a, b), and Marsh (1992a, b).

Alluvium samples were obtained from cores collected during drilling. Thin sections were prepared from grain mounts and analyzed petrographically with both optical and electron microscopy coupled with energy-dispersive spectroscopy. These methods determined that the alluvium is composed of plagioclase (andesine), quartz, orthoclase, a calcium- and iron-rich amphibole, biotite, magnetite, and ilmenite grains. Microscopy also identified iron oxide coating on grains and, probably, maghemite, γ-Fe_2O_3, an alteration of magnetite. Small, 2- to 5-mm crystals of chalcopyrite were also found. X-ray diffraction of the clay-size fraction indicates that the major clay minerals are kaolinite, mica, and smectite, with minor amounts of vermiculite, goethite and hematite. Microscopy indicates that manganous ilmenite comprises about 0.2 percent of the aquifer alluvium. The ilmenite $(Fe_{1.0-0.8},Mn_{0.0-0.2})TiO_3$ contains from about 0 to 20 percent manganese substituting for iron in a solid solution with pyrophanite, $MnTiO_3$. The ilmenite is being altered to leucoxene (a combination of rutile, TiO_2; anatase, TiO_2; and sphene, $CaTiO(SiO_4)$). Additional results of the solid-phase part of this study were reported by Troester and others (1990a, b).

Guillou and Glass (1957) studied the beach sands of Puerto Rico. In the heavy mineral fraction of their samples from the beach along the Valle de Yabucoa they found magnetite, pyroxene (augite), epidote, sphene, garnet, clinozoisite, zircon, and chlorite (listed in approximate relative abundance from most abundant to least).

Marsh (1992a, b) collected and semi-quantitatively analyzed stream sediment samples from Puerto Rico. Of the 2,852 chemical analyses reported, 22 were for sites within the Yabucoa or Punta Guayanés quadrangles. Table 1 lists the minimum, maximum, and average chemical concentration of selected x 10 elements for these 22 samples.

The soils developed on the alluvium belong to the Coloso-Toa-Bajura association. These are deep, moderately well drained to poorly drained, nearly level soils on flood plains. The soils range in composition from clay to silty clay to silty clay loam (Boccheciamp, 1977).

Climate

The average annual temperature of Puerto Rico is about 25°C. Nearly constant easterly trade winds occur across the island. Precipitation is measured daily at about 70 weather stations, and temperature and pan evaporation are measured at about 20 and 8 stations, respectively. Precipitation patterns in Puerto Rico are a result of the orographic effect of the central mountains on the easterly trade winds. Tropical storms and hurricanes occasionally strike the island, but more often they pass at some distance. The anomalously high wind and rain generated by the passage of these storms through the vicinity of Puerto Rico can affect the island for several days. The average annual precipitation varies across the island and ranges from more than 4,000 mm in a rain forest in the northeast, to less than 900 mm along most of the southern coast.

Table 1. Minimum, maximum, and average chemical concentrations for the 22 stream sediment samples in the Yabucoa and Punta Guayanés quadrangles from Marsh (1992a, b)

[<, less than; µg/g, micrograms per gram]

Element	Minimum		Maximum		Average	
Calcium (Ca)	1	weight percent	5	weight percent	2.3	weight percent
Iron (Fe)	1.5	weight percent	10	weight percent	6.5	weight percent
Magnesium (Mg)	0.2	weight percent	1.5	weight percent	1.0	weight percent
Sodium (Na)	1	weight percent	5	weight percent	1.9	weight percent
Phosphorus (P)	< 0.2	weight percent	< 0.2	weight percent	< 0.2	weight percent
Titanium (Ti)	0.3	weight percent	1	weight percent	0.5	weight percent
Silver (Ag)	< 0.5	µg/g	< 0.5	µg/g	< 0.5	µg/g
Arsenic (As)	< 200	µg/g	< 200	µg/g	< 200	µg/g
Boron (B)	< 10	µg/g	< 10	µg/g	< 10	µg/g
Barium (Ba)	200	µg/g	1,500	µg/g	780	µg/g
Beryllium (Be)	< 1	µg/g	1	µg/g	< 1	µg/g
Bismuth (Bi)	< 10	µg/g	< 10	µg/g	< 10	µg/g
Cadmium (Cd)	< 20	µg/g	< 20	µg/g	< 20	µg/g
Cobalt (Co)	< 10	µg/g	50	µg/g	23	µg/g
Chromium (Cr)	10	µg/g	200	µg/g	50	µg/g
Copper (Cu)	15	µg/g	50	µg/g	34	µg/g
Gallium (Ga)	50	µg/g	70	µg/g	54	µg/g
Germanium (Ge)	< 10	µg/g	< 10	µg/g	< 10	µg/g
Lanthanum (La)	< 50	µg/g	50	µg/g	< 50	µg/g
Manganese (Mn)	300	µg/g	1,500	µg/g	1,130	µg/g
Molybdenum (Mo)	< 5	µg/g	< 5	µg/g	< 5	µg/g
Niobium (Nb)	< 20	µg/g	< 20	µg/g	< 20	µg/g
Nickel (Ni)	< 5	µg/g	30	µg/g	10	µg/g
Lead (Pb)	10	µg/g	100	µg/g	27	µg/g
Antimony (Sb)	< 100	µg/g	< 100	µg/g	< 100	µg/g
Scandium (Sc)	5	µg/g	30	µg/g	22	µg/g
Tin (Sn)	< 10	µg/g	20	µg/g	< 10	µg/g
Strontium (Sr)	200	µg/g	500	µg/g	310	µg/g
Thorium (Th)	< 100	µg/g	< 100	µg/g	< 100	µg/g
Vanadium (V)	50	µg/g	1,500	µg/g	490	µg/g
Wolfram (W)	< 20	µg/g	< 20	µg/g	< 20	µg/g
Yttrium (Y)	< 10	µg/g	70	µg/g	37	µg/g
Zinc (Zn)	< 200	µg/g	200	µg/g	< 200	µg/g
Zirconium (Zr)	150	µg/g	> 1,000	µg/g	480	µg/g
Gold (Au)	< 0.002	µg/g	0.3	µg/g	0.017	µg/g

The National Oceanic and Atmospheric Administration maintains one meteorological station in the study area at the Central Roig in about the center of the Valle de Yabucoa. The station is operated daily by the Puerto Rico Sugar Corporation and is officially named Yabucoa 1 NNE, Puerto Rico (669829). The yearly annual precipitation, average annual temperature, and annual pan evaporation for this station for some recent years with nearly complete data are listed in table 2. The average annual precipitation was reported by Calvesbert (1970) as 2,242 mm. More recently the Southeast Regional Climate Center reported the normal precipitation for the years 1961 to 1990 as 2,046 mm (Southeast Regional Climate Center, unpublished data, 1995). Precipitation generally increases in the higher altitudes to the west and decreases toward the ocean in the east.

Precipitation occurs throughout the year in Puerto Rico, but there is a relative dry season, usually lasting from January or February to March or April. Rainfall is usually heaviest in May, August, September, and October. The monthly normal precipitation values (1961-90) for the metrological station at the Central Roig are shown in figure 2. The

Southeast Regional Climate Center has calculated the normal annual average temperature at this metrological station for the years 1961-90 as 25.7 °C. The difference between the average temperature for the coldest months (23.9 °C in January and February) and the hottest month (27.2 °C in August) is less than 4 °C.
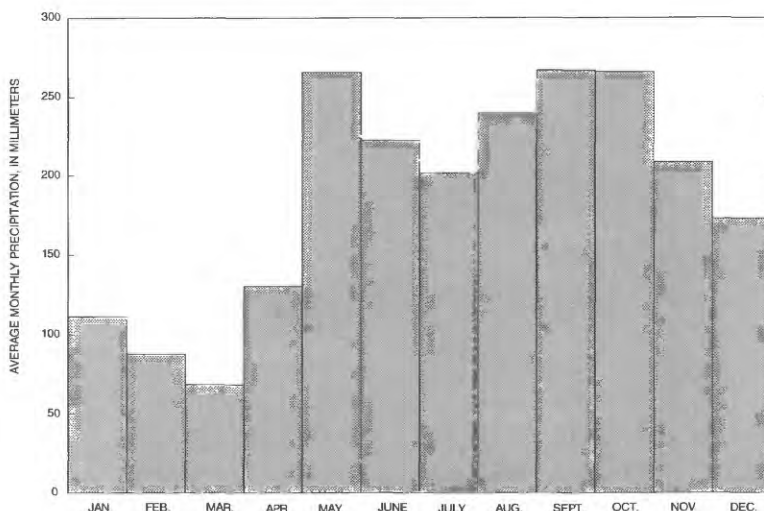
Figure 2. Precipitation histogram of the average monthly precipitation at the Central Roig, Yabucoa, Puerto Rico (from Calvesbert, 1970).

Table 2. Annual precipitation, average temperature, and annual pan evaporation for the National Oceanic and Atmospheric Administration weather station at Central Roig, in Yabucoa, Puerto Rico [na, not available]

Year	Annual precipitation, in millimeters	Average temperature, in degrees Celsius	Annual pan evaporation, in millimeters
1987	2,722	26.5	1,719
1988	2,056	na	1,805
1989	1,684	25.4	1,786
1990	1,452	25.7	1,765
1991	1,599	26.0	1,733
Average for 1987-91	1,903	25.9	1,762
Annual averages from Calvesbert (1970)	2,242	na	na
Climatological normals for 1961-90 (Southeast Regional Climate Center, unpublished data, 1995)	2,046	25.7	na

Little evaporation or evapotranspiration data exist for Puerto Rico. According to Calvesbert (1970), the potential evaporation at coastal stations exceeds the precipitation, while at interior stations the precipitation exceeds the potential evaporation. The average annual pan evaporation reported at the Central Roig for the years 1987-91 is 1,762 mm, which is about 93 percent of the average annual precipitation of 1,903 mm for the same 5-year period (table 2). However, pan evaporation is a measure of potential evaporation. Actual evapotranspiration is frequently less than the measured pan evaporation.

Giusti and López (1967) estimated annual evapotranspiration for a river basin west of Yabucoa, the Río Grande de Patillas Basin. In that basin, they derived a value for evapotranspiration from the drainage area (65 km^2), the average precipitation (1,905 mm), and the average discharge (3.94 m^3/s) at the Río Grande de Patillas at Patillas, USGS Station 50094200. The value they determined for evapotranspiration was about 760 mm or about 40 percent of the precipitation. The value for evapotranspiration in the Valle de Yabucoa may be similar to this amount, which is less than the reported annual pan evaporation. The 40 percent value is in agreement with previous studies of the hydrology of the area (Anders, 1971; Robison and Anders, 1973), which assumed that evapotranspiration was about 50 percent of precipitation.

Geomorphology (Landforms and Drainage)

The altitude of the hills surrounding the Valle de Yabucoa reaches a maximum of about 650 m at the head of the Río Guayanés basin. The land surface in the Valle de Yabucoa slopes gently from an altitude of about 30 m above mean sea level at western edge of the valley to sea level where the valley meets the Caribbean Sea. The hills flanking the valley and the material underlying the alluvium within the valley consist of the San Lorenzo Batholith and related rocks.

The Río Guayanés, with a drainage area of 88 km^2, is the largest stream flowing through the Valle de Yabucoa. The study area is also drained by the Caño de Santiago, the Río del Ingenio, the Río Limones, and several smaller streams. Large floods, such as the one that occurred on September 6, 1960, with the near passage of Hurricane Donna, flooded almost the entire Valle de Yabucoa (Fields, 1971). Floods of this magnitude are infrequent.

During the Pleistocene, sea level was as much as 120 m lower than it is today (Fairbanks, 1989). At that time the Río Guayanés cut a deep valley into the underlying bedrock as the stream eroded down toward base level. The paleovalley of the Río Guayanés and its principal tributaries was not only much deeper than the present valley, but the valley surface was much more irregular. Ridges now partly or completely buried extended far out into the valley, and isolated or semi-isolated hills rose rather abruptly from the valley floor. The location of one of these ridges, Harbor Ridge, is shown in figure 1.

As sea level began to rise to its current position, the valley was gradually filled by alluvial material, possibly behind a bay-mouth bar. In addition to alluvium there are swamp and beach deposits in the eastern part of the valley fill. Harbor Ridge probably existed as a peninsula, or as a peninsula and a small island, in the partly submerged valley. The island and at least the northern part of the ridge were completely covered by the sea when it rose higher. Presumably, the sea also occupied that part of the valley west and northwest of Yabucoa. Most of the alluvial material that filled the valley was derived from the surrounding hills. Harbor Ridge near the mouth of the valley probably acted as a barrier to the inland movement of sediments transported by sea currents.

As a result of shifts in the positions of the ancestral streams, periodic advances and retreats of the sea, and the presence of hills and ridges, the deposited thickness of alluvium and its grain-size distribution varies appreciably over short distances. Harbor Ridge is a major subsurface feature in the underlying bedrock topography that strongly influenced the geology and hydrology of this part of the valley and affected the amount of sand deposited in the overlying alluvium. According to Anders (1971), the southern half of the ridge is close to the surface, and the thickness of the overlying alluvium there is less than 3 m. From about its midpoint, the ridge declines to the northeast. Near the Caño de Santiago, the crest of the

ridge is about 15 m below sea level and only about 9 m above the adjacent ancestral valley floor. Along the northern half of the ridge, the effect of the ridge on the total thickness of alluvium is much less pronounced. The maximum thickness of the alluvium in the Valle de Yabucoa is not known, but it probably exceeds the 107 m penetrated by the deep observation well that was drilled as part of this study (Richards and Troester, 1991, 1993). The bottom of the alluvium is probably at or slightly above the minimum altitude of sea level during the Pleistocene, which was near 120 m below the current mean sea level (Fairbanks, 1989).

The contact between the top of the weathered San Lorenzo Batholith and the base of the alluvium forms an irregular erosional surface. According to Anders (1971), topographic relief on this ancient surface is known to exceed 12 m in a horizontal distance of less than 150 m at some places, but even greater relief may occur elsewhere. Excluding the effect of the buried ridges and taking the alluviated valley as a whole, these topographic irregularities may not be exceptionally important hydrologically. The partly or nearly completely buried ridges extending far out into the valley, however, may alter the subsurface hydrology significantly because the ridges form a partial barrier to the normal seaward movement of ground water. In addition, the Harbor Ridge, which is near the sea, appears to have appreciably delayed the inland movement of saline water as pumping lowered ground-water levels inland from the ridge.

METHODS

Drilling Methods

The USGS used an air-rotary drilling rig with a hollow stem auger to install wells up to 60 m deep at eight locations in the Valle de Yabucoa. Most of the observation wells were constructed with 5-cm PVC casing, although three--Central Roig 1, Calabazas, and Playita 1--were constructed with 10-cm PVC casing. During drilling, samples of the aquifer material were collected by using a split spoon sampler in the middle of the hollow stem auger. Samples were usually collected from the surface down until the movement of

ground water carried fine sand into the hollow stem and caused the split spoon sampler to bind. Because of this problem, samples were seldom collected from more than 15 m below land surface.

A private contractor used a dual-tube, reverse air-rotary drilling system with an open-center bit to drill one well. With this drilling method, a large compressor forces air down the annulus between the dual-walls of the drill stem. The compressed air forces the drill cuttings, cores, and ground water into the open center of the bit where they are carried to the surface up the center of the drill stem. This method allows the specific conductance of the ground water to be measured without the interfering effects of drilling mud. The contractor constructed the observation well with 5-cm PVC casing.

Electromagnetic Surface Geophysics Methods

Two electromagnetic surface geophysical methods were used to determine the depth to bedrock, the approximate depth of the saline-freshwater interface, and aquifer characteristics. The terrain conductivity (TC) method was used as a reconnaissance tool because this method permits rapid data collection. Subsequently, the transient electromagnetic (TEM) method was used. Of the two methods, TEM method provides better vertical resolution and can penetrate to a greater depth.

Terrain Conductivity (TC) Method

The TC method is a dual loop profiling tool that can directly measure the apparent electrical conductivity of the ground. The depth to which this equipment can measure apparent electrical conductivity is limited to about 60 m (McNeill, 1991). The EM34-3, produced by Geonics, was used for this method. This equipment operates at frequencies of 400, 1,600, and 6,400 Hz and at coil separations of 10, 20, and 40 m. The wider coil separations use lower frequencies to probe to greater depths. In addition, the equipment can be used in either the vertical or horizontal dipole modes for each of the 10-, 20-, and 40-m coil separations. These coil orientating and coil separations provided six values of apparent

conductivity for each of 84 sites in the Valle de Yabucoa. A more detailed discussion of this equipment and techniques used can be found in McNeill (1980, 1983).

The six measurements of apparent conductivity obtained for each of the sites were analyzed using the EMIX34 computer program by Interpex. This program assumes a layered earth model and uses a set of user-defined values of layer conductivities and depths as a starting model for each site. A synthetic curve is computed by the program from the starting model. Once the field data are plotted as conductivities and thicknesses versus depth, the program tries to find the best fit between the field data and a synthetic curve. The result is a one-dimensional geoelectric model at each data-collection site.

Transient Electromagnetic (TEM) Method

The TEM method measures the time-decay curve of an induced electromagnetic field. The decay curve can be transformed into a one-dimensional geoelectric model of the changes in conductivity with depth using interpretation software (McNeill, 1991). This method can measure apparent electrical conductivity to a much greater depth than the TC method and, depending on the size of the transmitter loop, can operate to depths of up to a few kilometers. The equipment used in this part of the project, was the EM47 produced by Geonics with a square transmitter loop of 40 or 100 m on a side. The depth of penetration can be as much as twice the diameter of the transmitter loop. The use of two repetition frequencies in this study permitted the collection of 40 values of apparent conductivity for each of the 31 sites in the Valle de Yabucoa. The 40 m loop was used at 27 of these sites, and the 100-m loop was used in the remaining four sites. A more complete description of the physics of the TEM method can be found in Fitterman and Stewart (1986).

The data obtained for each of the sites were analyzed using the TEMIX47 computer program by Interpex. Similar to the EMIX34 program, this program also assumes a layered earth model, and uses a set of user-defined values of layer conductivities and depths as a starting model for each site. A synthetic curve is computed by the program from the starting model. Once the field data are plotted as conductivities

and thicknesses versus depth, the program tries to find the best fit between the field data and a synthetic curve.

Geochemical Methods

Water samples were collected from existing production and abandoned wells and from the new wells drilled as part of this investigation. Abandoned and new wells were sampled with submersible pumps following the evacuation of at least three well volumes of water. Production wells were sampled using the available pump.

Field measurements of water temperature and specific conductance were collected with a YSI Model 33 meter. Field measurements of pH and alkalinity were conducted with an Orion pH meter using procedures described by Wood (1976). Field Eh measurements were also collected with the Orion pH meter and an Eh probe, corrected using ZoBell solution, and following the procedures described by Wood (1976).

Water samples were collected, filtered through a 0.45 μm filter, acidified with nitric acid, refrigerated, and analyzed in the laboratory for calcium, magnesium, sodium, potassium, silica, iron, and manganese. Water samples were collected, filtered through a 0.45 μm filter, refrigerated, and analyzed for chloride, sulfate, and fluoride. Water samples were collected, filtered through a 0.45 mm filter, preserved with mercuric chloride, refrigerated, and analyzed for phosphate, nitrite, and nitrite plus nitrate. Water samples were collected, filtered through a 0.10 μm filter, acidified with nitric acid, refrigerated, and analyzed for aluminum. Water samples were collected, filtered through a 0.45 μm filter in a stainless steel filter unit, refrigerated, and analyzed for dissolved organic carbon. Water samples were collected, preserved with zinc acetate, refrigerated, and analyzed for hydrogen sulfide. All laboratory analyses were preformed by the U.S. Geological Survey National Water Quality Laboratory using methods described in detail by Fishman and Friedman (1989). Additionally, a Hach spectrophotometer and reagents were used in the field to measure iron, manganese, and dissolved oxygen colorimetrically.

Alluvium samples were obtained from cores collected during drilling. Thin sections were prepared from grain mounts and analyzed petrographically with both optical and electron microscopy coupled with energy-dispersive spectroscopy. The techniques of the solid-phase study were reported by Troester and others (1990a, b).

HYDROGEOLOGY OF THE VALLE DE YABUCOA ALLUVIAL AQUIFER

The Valle de Yabucoa alluvial aquifer is composed of yellowish-brown to medium-gray sand, silt, and clay with occasional pebbles, cobbles, and boulders eroded from the San Lorenzo Batholith and deposited in the paleovalley of the Río Guayanés. The aquifer has a maximum thickness of more than 100 m, but is probably less than 120 m.

The hydrogeology of the Valle de Yabucoa alluvial aquifer has been previously described by Anders (1971) and Robison and Anders (1973). These studies were conducted when the main economic activity in the valley was the growing and processing of sugar cane and prior to the construction of the major industries now operating in the valley. Anders (1971) gives a detailed description of factors that influence the hydrogeology of the area. Robison and Anders (1973) report on the results of an analog model that was constructed to simulate the effects of long-term pumping.

The shape of the bedrock surface below the alluvium appears to partly control ground-water flow. Anders (1971, p. 16) discusses the Harbor Ridge and its effect on ground-water flow and states that this ridge "may appreciably delay the inland movement of saline-water if pumping lowers ground-water levels inland from the ridge." He went on to predict that any serious saline-water encroachment was likely to occur north of the Caño de Santiago, where the Harbor Ridge was not present (Anders, 1971, p. 46).

A pre-development potentiometric-surface map of the area modified from Anders (1971, p. 32) is shown in figure 3. The water table is usually less than 10 m below land surface, except where the water table has been lowered by pumping. The direction of ground-water flow is generally to the east.

Much of the ground-water recharge to the valley probably occurs by the direct infiltration of precipitation. Ground water is also recharged along the small alluvial fans which flank the valley. Some recharge occurs from streambed infiltration (Anders, 1971), though some stream reaches gain water rather than lose. Recharge probably also occurs directly from fractures in the bedrock surrounding and underlying the alluvial aquifer. Prior to ground-water development in the valley, most ground-water discharged directly to the ocean.

Anders (1971) reports seven values of specific capacity and transmissivity from aquifer tests at different wells completed in the alluvial aquifer. Transmissivity at these sites ranged from 20 to 340 m^2/d, and averaged about 130 m^2/d. Specific capacity ranged from 90 to 520 (m^3/d)/m of drawdown, and averaged about 290 (m^3/d)/m of drawdown.

Robison and Anders (1973) constructed an electrical analog model of the aquifer to simulate the effects of long-term pumping. Based on their model, at a ground-water pumping rate of about 6 m^3/s saline water would not reach theoretical production wells along the Zanja Barra for about 200 years. Unfortunately, the model did not consider the migration of highly mineralized water occurring nearer the production wells.

The wells in the Valle de Yabucoa alluvial aquifer that are discussed in this report are listed in tables 3 and 4. The location of each of these wells is shown on the map in figure 4.

Nineteen wells were drilled and installed as part of this investigation. Eighteen of the wells were drilled by the USGS and one well was drilled by a private contractor. Drilling and construction data for the 19 wells are listed in table 4. Lithologic descriptions of the alluvium samples obtained at each of the eight drill sites are listed in tables 5 to 12. The locations of these wells are shown in figure 4.
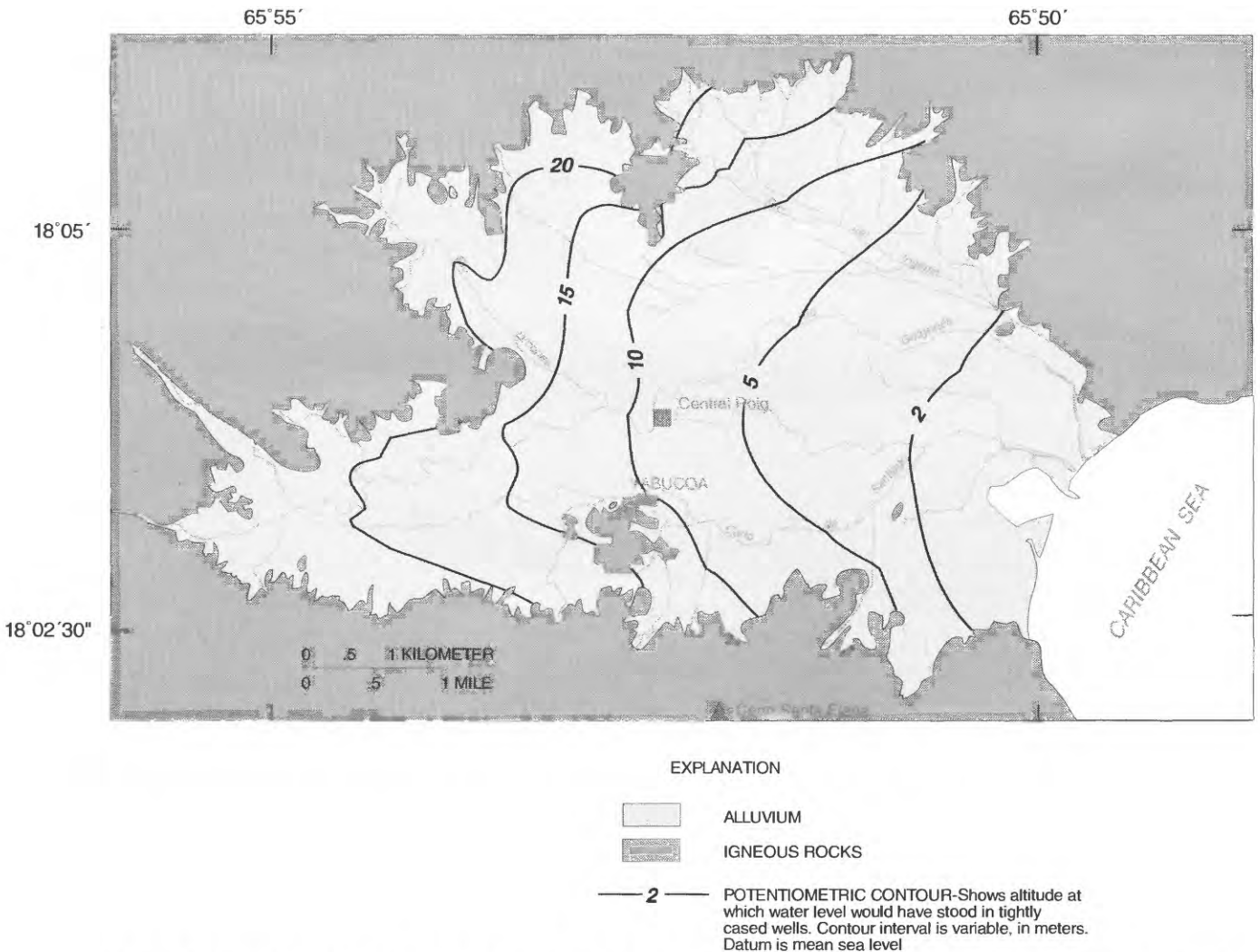
Figure 3. Pre-development potentiometric-surface map of the Valle de Yabucoa, Puerto Rico (modified from Anders, 1971, p. 32).

Table 3. Description of selected wells completed in the Valle de Yabucoa alluvial aquifer, Puerto Rico

[na, not available; PRASA, Puerto Rico Aqueduct and Sewer Authority]

Well number	Local well names	USGS Site ID	Other identifier	Use
1	Sun Oil #01 Well	180331065510600	03-65.50-06-08	Industrial water supply with large submersible pump
2	Sun Oil #02 Well	180336065511200	03-65.51-03-48	Industrial water supply with large submersible pump
3	Sun Oil #03 Well	180333065512900	03-65.51-02-46	Industrial water supply with large submersible pump
4	Sun Oil #04 Well	180344065513200	03-65.51-11-26	Not used at time of sampling. Subsequently used for industrial water supply
5	Sun Oil #06 Well	180403065513200	04-65.51-06-95	Industrial water supply with large submersible pump
6	Sun Oil #08 Well	180417065513400	04-65.51-03-75	Not used at time of sampling. Previously used for industrial water supply

Table 3. Description of selected wells completed in the Valle de Yabucoa alluvial aquifer, Puerto Rico--Continued

Well number	Local well names	USGS Site ID	Other identifier	Use
7	Union Carbide #1 Pozo Valle #07	180456065515100	04-65.51-01-02	Industrial water supply with turbine pump
8	Union Carbide #2 Pozo Valle #10	180442065515000	04-65.51-11-32	Industrial water supply with turbine pump
9	Union Carbide #3 Pozo Valle #13	180459065514100	04-65.51-15-04	Not used at time of sampling
10	Union Carbide #4 Pozo Valle #14	180459065514101	04-65.51-16-04	Industrial water supply with turbine pump
11	Union Carbide #5	180440065523200	na	Industrial water supply with turbine pump
12	Union Carbide #6 Pozo Valle #11	180456065514900	04-65.51-12-02	Industrial water supply with turbine pump
13	Pozo Calabazas	180330065550100	03-65.55-01-50	Public water supply with turbine pump
14	Central Roig Pozo Yabucoa #21	180351065525700	03-65.52-02-16	Industrial water supply with turbine pump
15	Pozo de la Grúa (PRASA)	180410065522900	04-65.52-09-85	Public water supply with turbine pump
16	Limones (PRASA) Pozo Central Roig	180358065523700	03-65.52-08-05	Public water supply with turbine pump
17	Viejo Roig (PRASA)	180344065523000	na	Public water supply with turbine pump
18	Guayanés (PRASA) Pozo Yabucoa	180416065501100	04-65.50-03-79	Public water supply with turbine pump
19	Test Well #08 Number 1	180416065530100	04-65.53-02-80	Not used at time of sampling.
20	Pozo Barrio Limones	180505065542200	05-65.54-01-97	Not used at time of sampling.
21	R.J. Reynolds #02 Pozo Valle # 24	180522065511800	05-65.51-02-68	Industrial water supply with turbine pump
22	R.J. Reynolds #03 Pozo Valle # 25	180524065511500	05-65.51-03-68	Industrial water supply with turbine pump
23	AH #02	180548065513700	05-65.51-05-14	Not used at time of sampling.
24	AH #03	180334065523300	03-65.52-13-45	Not used at time of sampling.
25	Pozo Martorell	180405065544300	04-65.54-01-30	Not used at time of sampling.
26	Manantial Rivera	180204065550100	02-65.55-01-80	spring
27	Manantial F. Rojas	180224065550900	02-65.55-02-69	spring
28	Manantial Rodríguez	180202065520800	02-65.52-02-49	spring
48	Pozo Yabucoa 7	180415065543900	04-65.51-05-74	USGS observation well with automatic digital recorder
49	Observation Well #1 TW-01	180349065502300	03-65.50-01-17	Abandoned
50	Observation Well #2 TW-01	180342065502300	03-65.50-04-27	Abandoned
51	Pozo Valle #1	180351065495700	03-65.49-02-11	Abandoned
52	Pozo Valle #6	180411065500900	04-65.50-02-89	Abandoned
53	Port Authority Well	180359065501301	03-65.50-07-08	Abandoned

Table 4. Observation wells installed for this study by the U.S. Geological Survey in the Valle de Yabucoa, Puerto Rico

Well number	Well name	USGS Site ID	Screened interval in feet below land surface	Total depth in feet below land surface
29	Central Roig 1	180358065523701	30 to 40	44
30	Central Roig 2	180358065523702	95 to 115	115
31	Calabazas	180330065550100	41 to 61	61
32	Playita 1	180250065542200	88 to 108	108
33	Playita 2	180250065542201	40 to 50	50
34	Martorell 1	180451065532601	20 to 35	35
35	Martorell 2	180451065532602	55 to 75	75
36	Limones 1	180436065524801	101 to 121	121
37	Limones 2	180436065524802	15 to 35	35
38	Limones 3	180436065524803	57 to 77	77
39	Juan Martín 1	180425065520801	150 to 170	170
40	Juan Martín 2	180425065520802	109 to 129	129
41	Juan Martín 3	180425065520803	16 to 36	36
42	Sun 1	180414065513200	32 to 52	52
43	Sun 2	180414065513201	168 to 188	188
44	Harbor 1	180344065505001	79 to 99	99
45	Harbor 2	180344065505002	17 to 37	37
46	Harbor 3	180344065505003	125 to 145	145
47	Deep observation well	180358065503600	330 to 340	350
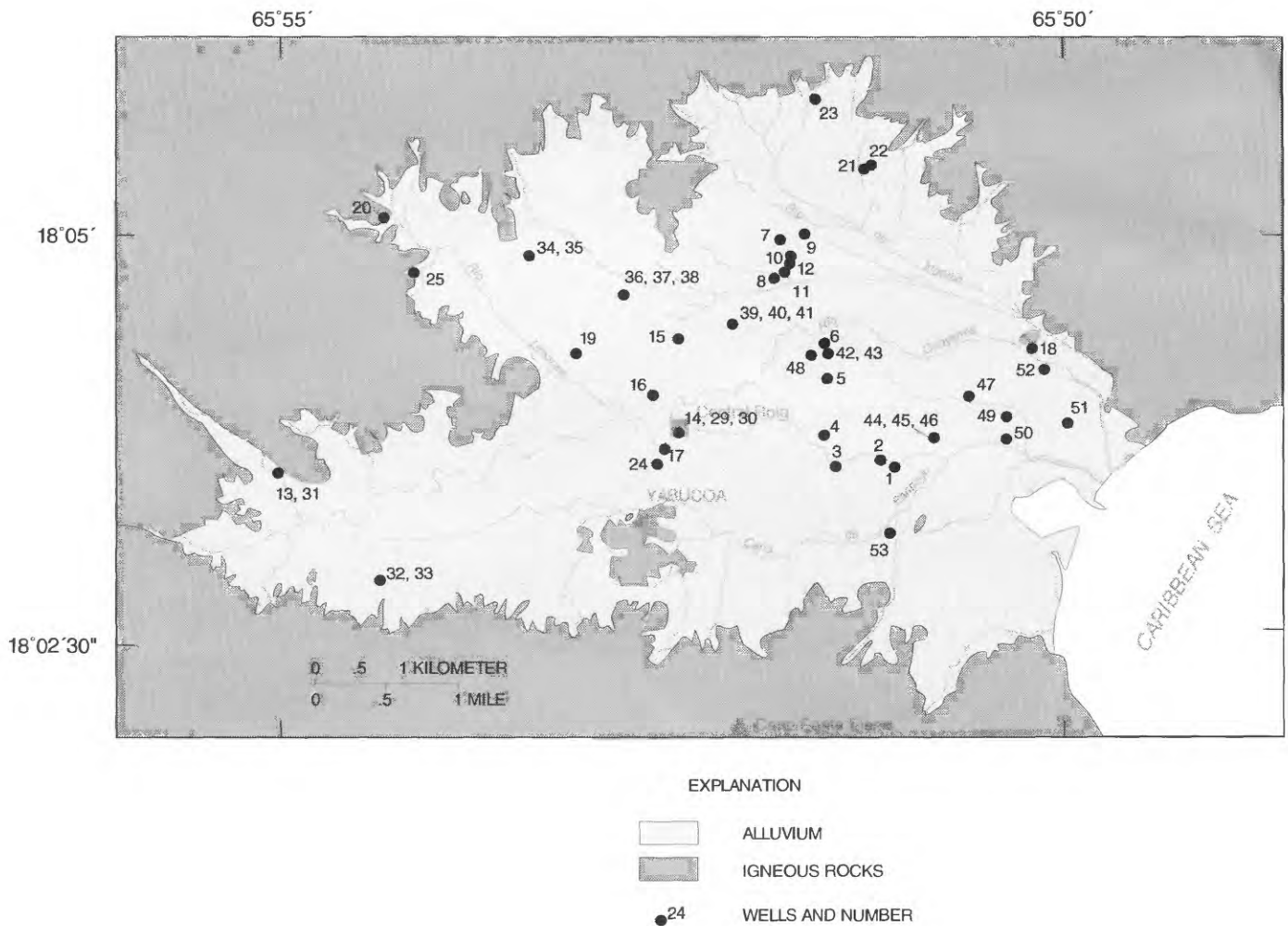
Figure 4. Locations of selected wells in the Valle de Yabucoa, Puerto Rico.

Table 5. Lithologic description of alluvium samples obtained at the Central Roig drill site, Valle de Yabucoa, Puerto Rico

Depth below land surface, in feet	Lithologic Description
0 to 4	grayish-black clay
4 to 9	grayish-olive-green clay
9 to 14	light-olive-brown, medium sand
14 to 19	grayish-black, medium to coarse sand
19 to 24	moderate-olive-brown, fine sand
24 to 29	moderate-olive-brown clay
29 to 34	moderate-olive-brown, poorly sorted, medium to very coarse sand
34 to 39	moderate-brown clay
39 to 44	moderate-yellowish-brown, sandy clay
44 to 49	moderate-brown, sandy clay
49 to 54	moderate-brown, sandy clay
54 to 59	moderate-yellowish-brown, medium sand
59 to 64	light-brown, medium sand with some clay
64 to 69	moderate-yellowish-brown, coarse sand
69 to 74	moderate-yellowish-brown, fine sand

Table 6. Lithologic description of alluvium samples obtained at the Calabazas drill site, Valle de Yabucoa, Puerto Rico

Depth below land surface, in feet	Lithologic Description
0 to 4	clay with medium sand
4 to 9	medium to fine sand with silt and clay
9 to 14	poorly sorted, medium sand
14 to 19	coarse sand with pebbles
19 to 24	very coarse sand with some clay
24 to 29	medium to coarse sand
29 to 34	stiff clay
34 to 39	stiff clay
39 to 44	fine to very fine sand
44 to 49	medium sand
49 to 54	very stiff clay
54 to 59	medium sand with interbedded clay
59 to 64	coarse sand

Table 7. Lithologic description of alluvium samples obtained at the Playita drill site, Valle de Yabucoa, Puerto Rico

Depth below land surface, in feet	Lithologic Description
0 to 4	dark-yellowish-brown, poorly sorted, coarse sand
4 to 9	moderate-yellowish-brown, poorly sorted, coarse sand
9 to 14	moderate-yellowish-brown, poorly sorted, coarse sand
14 to 19	dark-yellowish-brown, poorly sorted, coarse sand
19 to 24	light-brown, medium sand with silt and clay
24 to 29	moderate-yellowish-brown, medium sand with clay
29 to 34	moderate-yellowish-brown, medium to coarse sand
34 to 39	pale-yellowish-brown, medium sand
39 to 44	stiff clay with medium to coarse sand
44 to 49	moderate-brown, very poorly sorted, medium sand with clay
49 to 54	moderate-brown, very poorly sorted, coarse sand with clay
54 to 59	no samples
59 to 64	moderate-yellowish-brown clay with medium to fine sand

Table 8. Lithologic description of alluvium samples obtained at the Martorell drill site, Valle de Yabucoa, Puerto Rico

Depth below land surface, in feet	Lithologic Description
0 to 4	moderate yellowish brown poorly sorted medium sand
4 to 9	moderate yellowish brown medium sand
9 to 14	medium gray very fine sand, silt, and clay
14 to 19	light bluish gray poorly sorted coarse sand
19 to 24	no samples
24 to 29	medium light gray coarse sand
29 to 34	medium light gray coarse sand
34 to 39	medium gray coarse sand
39 to 44	brownish gray coarse sand

Table 9. Lithologic description of alluvium samples obtained at the Limones drill site, Valle de Yabucoa, Puerto Rico

Depth below land surface, in feet	Lithologic Description
0 to 4	grayish-orange, medium sand
4 to 9	medium-dark-gray, medium to coarse sand
9 to 14	medium-dark-gray, medium to coarse sand
14 to 19	medium-gray, medium to coarse sand

Table 10. Lithologic description of alluvium samples obtained at the Juan Martín drill site, Valle de Yabucoa, Puerto Rico

Depth below land surface, in feet	Lithologic Description
0 to 4	moderate-yellowish-brown, poorly sorted, angular, medium sand
4 to 9	dark-yellowish-orange, poorly sorted, medium to coarse sand
9 to 14	olive-gray, poorly sorted, medium sand to clay
14 to 19	olive-gray, poorly sorted, medium sand to clay
19 to 24	medium-dark-gray, medium to coarse sand

Table 11. Lithologic description of alluvium samples obtained at the Sun drill site, Valle de Yabucoa, Puerto Rico

Depth below land surface, in feet	Lithologic Description
0 to 4	dark-yellowish-brown, very poorly sorted, coarse sand
4 to 9	moderate-yellowish-brown, medium to fine sand
9 to 14	dark-gray, medium to coarse sand
14 to 19	dark-gray, medium to coarse sand
19 to 24	grayish-green clay with medium sand
24 to 29	grayish-green, medium sand
29 to 34	dark-greenish-gray, medium sand with clay
34 to 39	medium-dark-gray, coarse sand
39 to 44	medium-gray, medium to coarse sand
44 to 49	medium-dark-gray, medium to coarse sand

Table 12. Lithologic description of alluvium samples obtained at the Harbor drill site, Valle de Yabucoa, Puerto Rico

Depth below land surface, in feet	Lithologic Description
0 to 4	dark-yellowish-brown, fine sand with clay
4 to 9	greenish-black, medium to coarse sand
9 to 14	dark-greenish-gray to black, stick, wet clay
14 to 19	dark-greenish-gray, medium to coarse sand
19 to 24	dark-greenish-gray, medium to coarse sand

In addition to the 18 wells drilled by the USGS, a 107-m-deep observation well was drilled by a private contractor into the deepest part of the paleochannel to monitor the movement of saline water into the aquifer on a long-term basis. The site for this well (fig. 4) was selected based on three criteria, the greatest depth to bedrock, likelihood of encountering saline water, and accessibility by the drill rig. Construction details for this well are included in table 4 and lithologic description of alluvial samples and the specific conductance of ground water obtained during drilling are in table 13.

Table 13. Lithologic description of alluvium samples and specific conductance of ground water obtained during drilling at the saline observation well drill site, Valle de Yabucoa, Puerto Rico

[nd, not determined]

Depth below land surface, in feet	Specific conductance, in µS/cm	Lithologic Description
0 to 10	nd	moderate-brown clay with some sand
10 to 20	nd	moderate-brown sand with black clay
20 to 30	290	black sand
30 to 40	nd	black sand and clay
40 to 50	nd	black sand and clay with 50 mm conch shell
50 to 60	600	black sand and clay
60 to 70	590	black to moderate-brown sand and clay
70 to 80	540	moderate-brown sand
80 to 90	500	moderate-brown coarse sand and clay
90 to 100	470	no samples
100 to 110	520	light-brown sand
110 to 120	540	light-brown to dusky-brown sand with very-coarse quartz pebbles
120 to 130	490	light-brown sand with very-coarse pebbles
130 to 140	480	light-brown sand and pebbles
140 to 150	490	light-brown sand and pebbles
150 to 160	500	moderate-brown sand
160 to 170	490	light-brown sand with light-brown to grayish-brown clay
170 to 180	510	grayish-brown to light-brown sand and clay
180 to 190	540	well sorted moderate-brown to grayish-brown sand with some pebbles
190 to 200	490	well sorted moderate-brown sand
200 to 210	590	poorly sorted moderate-brown sand with stiff, light-brown clay
210 to 220	580	grayish-brown to moderate-brown sand with clay layers
220 to 230	610	well sorted dusky-brown sand with quartz pebbles and coarse-pebble sized rock fragments
230 to 240	680	well sorted moderate-brown sand with some pebbles
240 to 250	690	moderate-brown sand and clay
250 to 260	830	moderate-brown sand and clay
260 to 270	910	well sorted moderate-brown sand
270 to 280	940	moderate-brown to dusky-brown sand with some clay layers
280 to 290	990	brownish-gray sand with some interbedded clay
290 to 300	1,040	hard moderate-reddish-brown clay and moderate-brown medium to coarse sand and clay with pebble-sized rock fragments
300 to 310	970	light-brown medium to coarse sand and pebbles with moderate-green clay layers
310 to 320	1,010	light-brown medium to coarse sand with pebbles, some well cemented sands
320 to 330	990	moderate-brown medium to fine sand with pebbles and with some interbedded clay
330 to 340	1,660	dusky-brown to moderate-brown to moderate-olive-brown medium sand with some clay layers, well-cemented sand layers, and very coarse granodiorite pebbles
340 to 350	3,500	moderate-olive-brown sand with pebbles and small cobbles and some clay layers

The deep observation well did not penetrate the consolidated granodiorite, but the well did penetrate the saprolite on top of the bedrock. This is the deepest well in the Valle de Yabucoa. The specific conductance of the water pumped to the land surface as the drill rig progressed through the alluvium revealed continuous freshwater with specific conductance values that fluctuated but remained below 700 µS/cm until about 75 m below land surface when the specific conductance began to rise to about 1,000 µS/cm. At about 100 m below land surface the specific conductance rose sharply to about 3,500 µS/cm. The well is constructed with a 6.1-m screen centered at 101 m below land surface. After casing, the water pumped from the well had a specific conductance that exceeded 10,000 µS/cm or about 20 percent of the specific conductance of sea water and more than ten times higher than the average specific conductance found elsewhere in the aquifer. The difference between the specific conductance values during drilling and after casing the well are due to the mixing of water of different specific conductance values during the drilling process. The land surface was estimated from topographic contours and a nearby highway survey to be about 0.8 m above mean sea level.

WATER USE FROM THE VALLE DE YABUCOA ALLUVIAL AQUIFER

Water Use

Ground-water withdrawals for industrial use from the Valle de Yabucoa alluvial aquifer increased with the construction of the refinery and the cigarette and graphite manufacturing plants in the 1970's. Ground-water withdrawal data for the refinery from 1978 through 1995 (fig. 5) are available from the Franchise Office of the Puerto Rico Department of Natural and Environmental Resources. No other consistent ground-water withdrawal data are available. Monthly average ground-water levels at the Yabucoa 7 observation well (number 48 in table 3 and fig. 4) and individual measurements of the ground-water level in the deep observation well installed for this project are also plotted in figure 5.
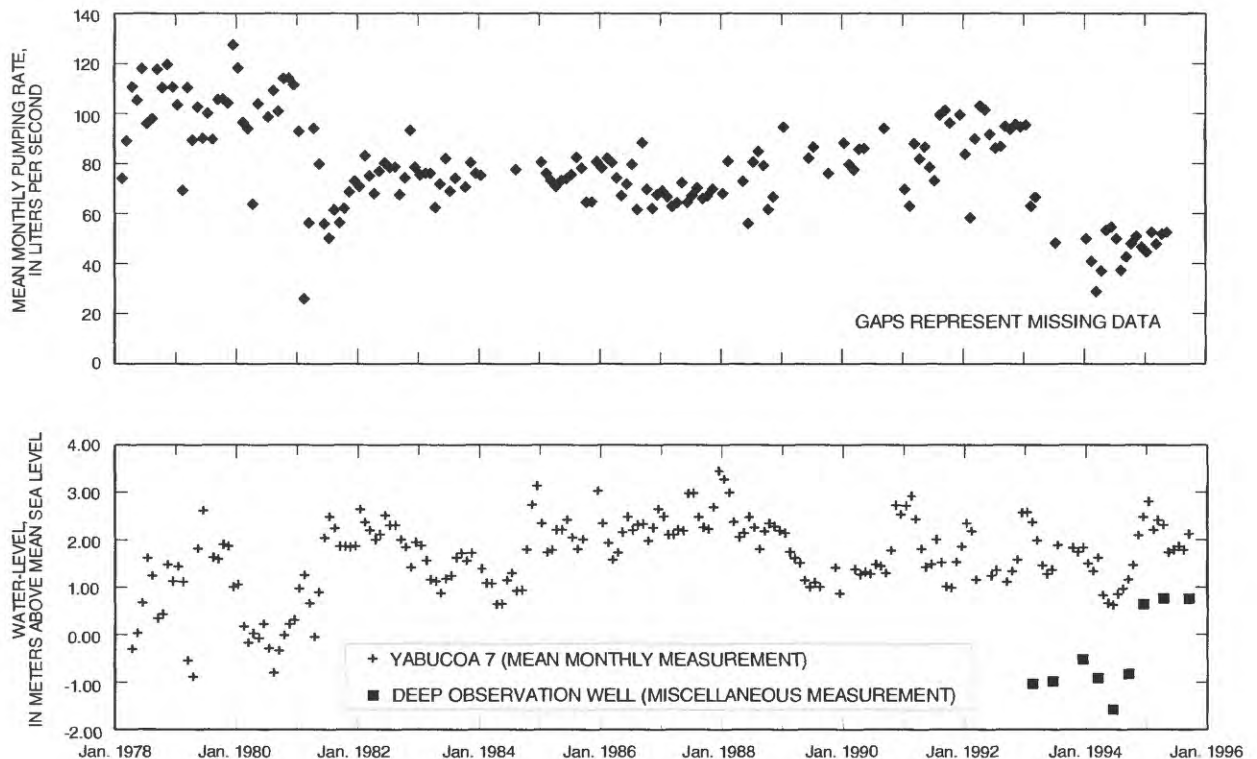
Figure 5. Pumping rate at the refinery and water levels in the Valle de Yabucoa alluvial aquifer in southeastern Puerto Rico.

The water levels in the Yabucoa 7 observation well and the deep observation well appear to respond to changes in pumping reported by the refinery (fig. 5). These two wells are closer to the pumping center for the refinery than they are to any of the other pumping centers in the valley. During 1978 to 1980, the refinery averaged more than 100 L/s of ground-water withdrawals. During this period the monthly average ground-water level at the Yabucoa 7 observation well frequently dropped below mean sea level. At the end of 1980, the refinery reduced their average withdrawal rate to about 75 L/s. Since that time the average water level at the Yabucoa 7 observation well has not been below mean sea level. In 1993, the refinery again decreased their withdrawals to an average of less than 50 L/s. This decrease in pumping occurred during a widespread drought in Puerto Rico that extended from about August 1993 to about December 1994 (U.S. Geological Survey, 1994-96). Water levels did not appear to recover in the deep observation well until the beginning 1995. The water level in the deep observation well was below mean sea level every time the water level was measured from when the well was constructed in February 1993 until September 1994. During that time the water level averaged about 1.0 m below mean sea level. Since December 1994 the water levels have risen and they average about 0.7 m above mean sea level (December 1994 to September 1995). The individual measurements for the deep observation well are tabulated in table 14.

Water level rises similar to the one observed in the deep observation well were observed in five other wells in the lower part of the Valle de Yabucoa alluvial aquifer. Each of these wells recorded a rise of more than 1 m from between 1991 and 1995. The water-level data are listed in table 15.

Potentiometric Surfaces

On July 5, 1990, stream-discharge and water-level data were collected at 21 sites along streams and numerous wells throughout the valley to define the extent of the cone of depression in the water table. The estimated potentiometric surface of the aquifer (fig. 6) is modified from Collar and others (1990). The observed base of the cone of depression produced by the pumping wells is 12 m below mean sea level. In addition, the potentiometric surface appears to be below mean sea level everywhere between the pumping wells and the ocean.

Table 14. Ground-water altitude and water specific conductance at the deep observation well in the Valle de Yabucoa, Puerto Rico

[nd, not determined]

Date	Ground-water altitude, in meters below land surface datum	Ground-water altitude, in meters above mean sea level	specific conductance, in microsiemens per centimeter at 25 °Celsius
February 19, 1993	1.83	-1.0	11,400
June 29, 1993	1.77	-1.0	10,700
December 27, 1993	1.32	-0.5	11,900
March 17, 1994	1.71	-0.9	12,000
June 22, 1994	2.37	-1.6	11,800
September, 13, 1994	1.62	-0.8	11,400
December 30, 1994	0.16	0.6	11,500
April 12, 1995	0.04	0.8	12,400
September 13, 1995	0.04	0.8	nd

Table 15. Ground-water altitude in 1991 and 1995 at 5 wells in the lower Valle de Yabucoa, Puerto Rico

Well number	Local well name	Date of water-level measurement in 1991	Water level in 1991, in meters below land surface datum	Date of water-level measurement in 1995	Water level in 1995, in meters below land surface datum	Rise in water level from 1991 to 1995, in meters
49	Observation Well #1 TW-01	January 3	1.30	November 7	0.26	1.04
50	Observation Well #2 TW-01	January 3	1.20	November 7	0.05	1.15
51	Pozo Valle #1	August 1	2.90	November 7	1.24	1.66
52	Pozo Valle #6	May 13	6.37	November 7	3.25	3.12
53	Port Authority Well	August 1	3.47	November 7	2.29	1.18

EXPLANATION

ALLUVIUM

IGNEOUS ROCKS

—— *15* —— POTENTIOMETRIC CONTOUR-Shows altitude at which water level would have stood in tightly cased wells. Contour interval is variable. Datum mean sea level
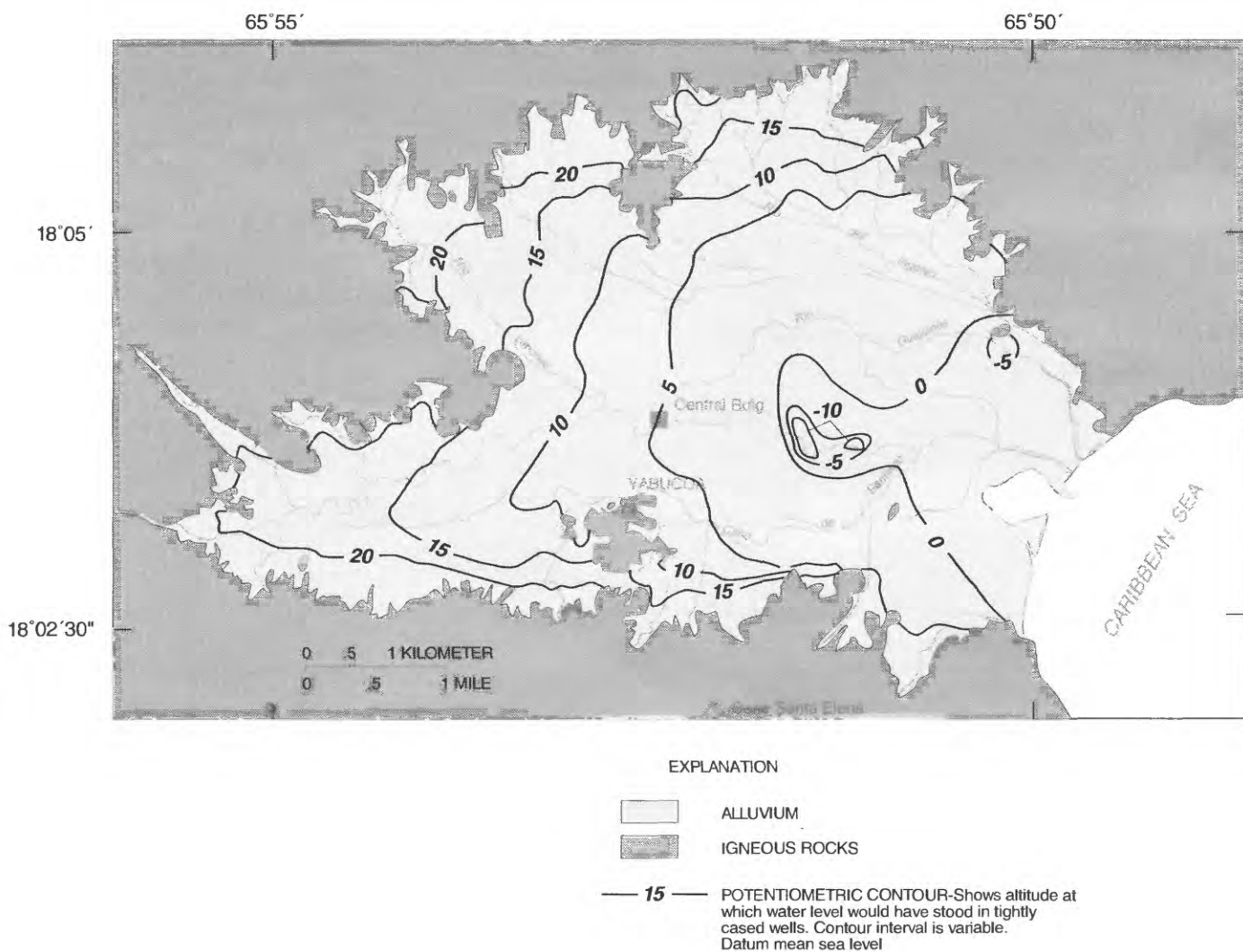
Figure 6. Potentiometric-surface map of the Valle de Yabucoa alluvial aquifer, Puerto Rico, July 1990.

Based on the 21 stream discharge measurements (see table 16 and fig. 7), there is no significant exchange of water between the aquifer and the streams and rivers that flow above it. The amount of water flowing across the middle of the valley (sites 6, 7, 24, 25, 36, 40, and 46) is within 1 percent of the amount that flows into the ocean (sites 38 and 48). For flowing streams to cross a cone of depression with no measurable effect on the streams or on the cone of depression indicates that there is no hydraulic connection between the surface- and ground-water systems.

Downstream of its confluence with the Río Limones, the Río Guayanés transported 75 percent of the surface water in the valley on the day of the seepage run. The Río Guayanés, to within the errors of measurement, probably has little or no exchange of water with the aquifer. The uncertainty of the conservation of mass calculations is increased by the fact that, on the day of the seepage run, the river stage, as measured at the vehicular bridge below Central Roig, fell 18 mm in 3.4 hours during the afternoon.

Table 16. Stream discharge data at selected sites in the Valle de Yabucoa, Puerto Rico on July 5, 1990
[m^3/s, cubic meters per second; nd, not determined]

Site number	Site name	Measured discharge, in m^3/s	Gains (+) or loses (-) in m^3/s
6	Río Limones above Río Guayanés	[a]0.348	nd
7	Río Guayanés above Río Limones	0.841	nd
8	Río Guayanés at Highway 3 (at noon)	1.090	nd
8	Río Guayanés at Highway 3 (in afternoon)	1.031	nd
24	Unnamed stream north of Río del Ingenio at Highway 3	[a]0.007	nd
25	Río del Ingenio at Highway 3	0.053	nd
27	Río del Ingenio above unnamed stream at Highway 906	0.076	-0.071
28	Río del Ingenio below unnamed stream at Highway 906	0.105	0.008
29	Río del Ingenio above Río Guayanés	0.092	-0.013
29	Río del Ingenio above Río Guayanés (repeat measurement)	[a]0.120	nd
30	Río Guayanés at Pozo Guayanés	1.164	0.062
32	Río Guayanés below Yabucoa 7	1.102	0.074
33	Río Guayanés above Yabucoa 7	1.028	-0.108
34	Río Guayanés at Central Roig Truck Bridge	1.136	0.075
36	Unnamed stream south of Río del Ingenio at Highway 3	[a]0.021	nd
37	Caño de Santiago below refinery	0.104	-0.019
38	Caño de Santiago near Harbor Navigational Aid	0.099	-0.005
39	Caño de Santiago at refinery	0.116	0.022
40	Caño de Santiago at Highway 3	0.094	nd
41	Quebrada Laja	0.007	nd
46	Quebrada Aguacate above Río del Ingenio	0.087	nd
48	Río Guayanés below Río del Ingenio	[a]1.362	0.106
63	Río Guayanés below Río Limones	1.090	nd

[a] Poor measurement with an error of more than 8 percent.
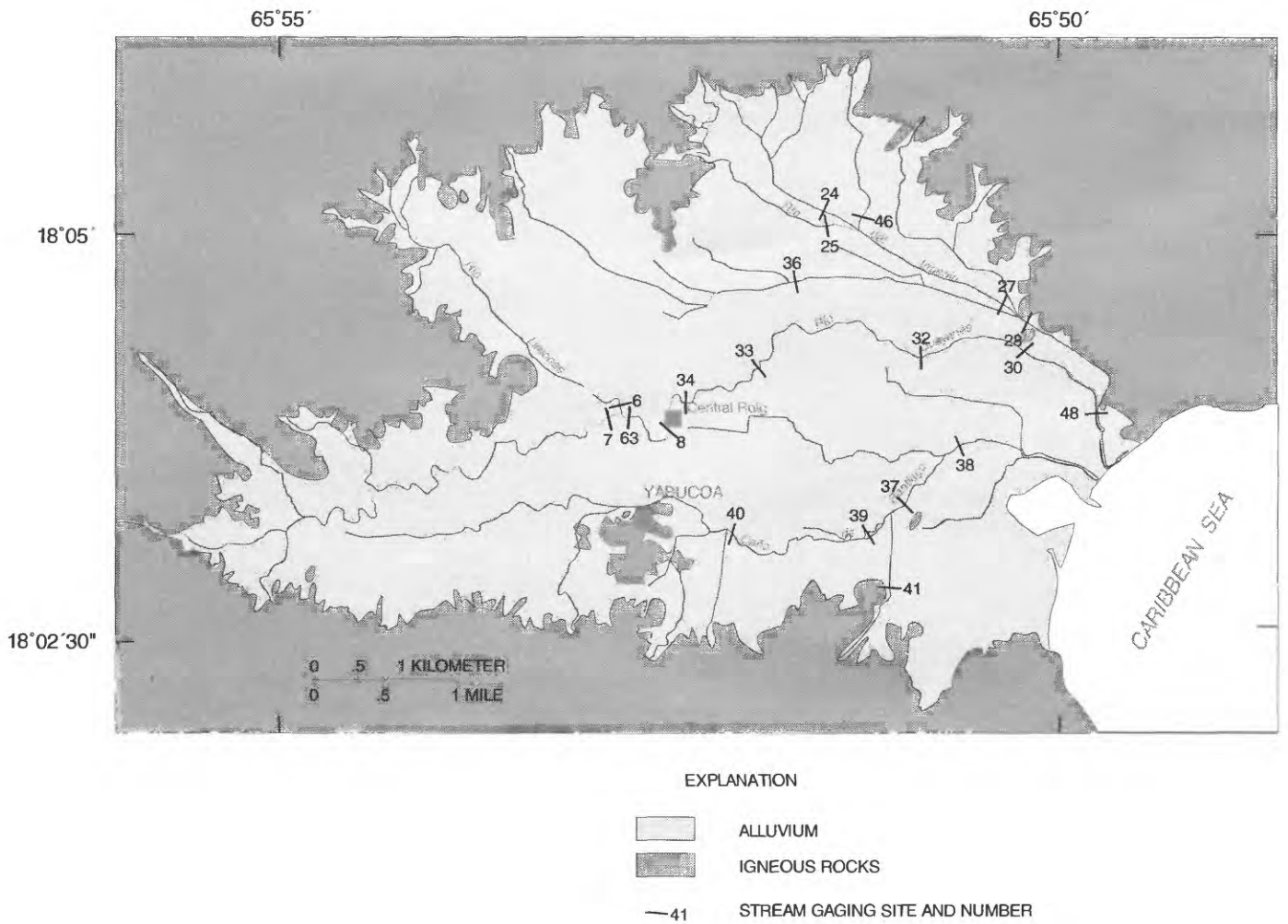
Figure 7. Location of the stream sites at which discharge measurements were made on July 5, 1990, in the Valle de Yabucoa, Puerto Rico.

The July 1990 potentiometric-surface map (fig. 6) can be compared with the pre-development potentiometric-surface (fig. 3) map from Anders (1971, p. 32). During July 1990, the largest cone of depression is L-shaped and centered over the wells that provide water to the refinery. A second, smaller cone is centered around the public supply well that is north of the Río Guayanés.

Under these conditions active saline-water encroachment into the alluvial aquifer could be occurring. The coalesced cones of depression from the pumping wells appear to have migrated to the ocean. Under these conditions, eventually saline water would likely arrive at the production wells.

With the post-1990 reduction of pumping for the refinery and the subsequent observed rise in the potentiometric surface at the deep observation well and other wells in the vicinity, a ground-water divide separating the ocean from the pumping wells has probably developed. If this is the case, the divide would likely prevent further inland migration of the saline water.
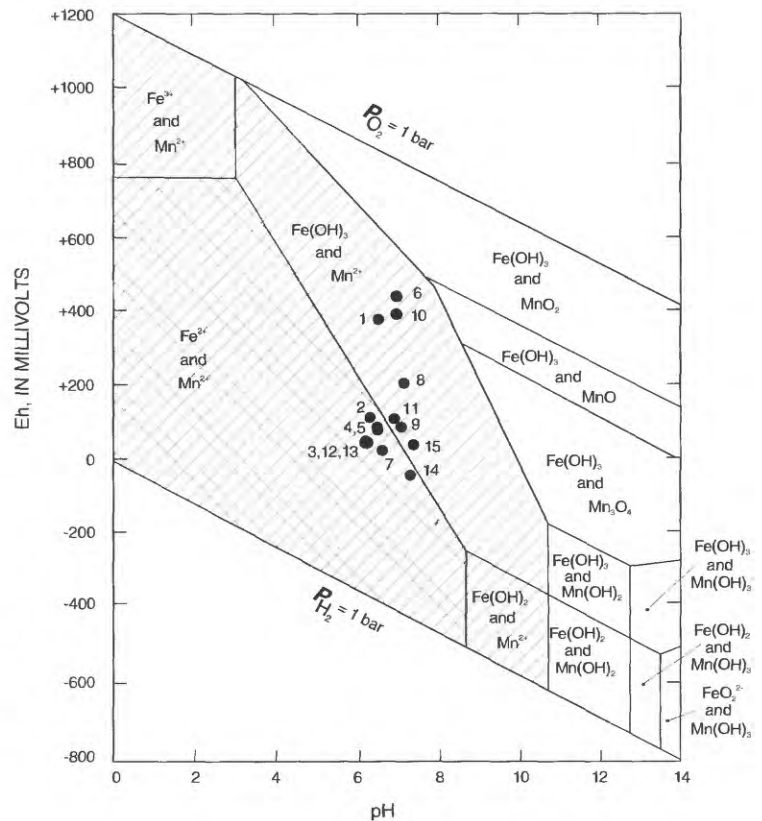
GEOCHEMISTRY OF THE VALLE DE YABUCOA ALLUVIAL AQUIFER

Iron and Manganese Chemistry

The results of the water-quality analyses are listed in table 17. Measured iron concentrations in the Valle de Yabucoa alluvial aquifer ranged from less than 0.003 to 28 mg/L, and manganese concentrations ranged from 0.016 to 3.6 mg/L. Although the elevated iron and manganese concentrations in the aquifer pose no health threat, they frequently exceed secondary standards for drinking water established by the U.S. Environmental Protection Agency of 0.3 mg/L for iron and 0.05 mg/L for manganese (U.S. House of Representatives, 1996).

Thermodynamics, including aqueous- and solid-phase equilibria and oxidation and reduction (redox) reactions, and kinetics are the geochemical processes that control the distribution of iron and manganese in ground water. The oxidation states of iron and manganese of hydrogeological significance are Fe^{2+}, Fe^{3+}, Mn^{2+}, and Mn^{4+}. The theoretical stable ranges of iron and manganese ions, oxides, and hydroxides as a function of Eh and pH are shown in figure 8. Oxidized iron, Fe^{3+}, is the dominant iron ion in solution only below a pH of about 3; oxidized manganese, Mn^{4+}, is never the dominant manganese ion in solution. The reduced species, Fe^{2+} and Mn^{2+}, are the dominant hydrated ions in solution in the Eh and pH range of natural waters. In much of the Eh and pH range of natural waters Fe^{3+} and Mn^{4+} form insoluble oxides or hydroxides. The Mn^{2+} ion is thermodynamically stable across a wider Eh-pH range than is the Fe^{2+} ion, as shown in figure 8. Consequently, the Mn^{2+} ion remains in solution in aqueous environments in which Fe^{2+} is oxidized to Fe^{3+} and precipitated as $Fe(OH)_3$.

The Eh, pH, and iron and manganese concentrations for water samples from the Valle de Yabucoa alluvial aquifer are plotted in figure 8 and listed in table 18. All of these samples are from wells drilled exclusively for monitoring purposes during this investigation. These chemical analyses agree with the theoretical predictions shown in the Eh-pH diagram. All of the water compositions that fall in the stability field of the Fe^{2+} ion have iron concentrations greater than 10 mg/L, whereas all the water compositions that

Figure 8. Eh-pH stability diagram for ferromagnesian oxides showing the Eh and pH of 15 ground-water samples from the Valle de Yabucoa alluvial aquifer, Puerto Rico. Iron and Manganese activities of 10^{-6} are assumed for the construction of the Eh-pH diagram. This diagram assumes that $Fe(OH)_3$ is the stable phase for the Fe(III) precipitate.

fall in the stability field for $Fe(OH)_3$ have iron concentrations that are less than 0.2 mg/L.

None of the samples plotted in figure 8 have Eh-pH combinations that plot within the stability field of MnO_2; however, it is possible that in high-production wells the redox potential is sufficiently elevated as a result of oxygenation and that the water composition would plot within the stability field of manganese dioxide. If this were the case then the Mn^{2+} ion should oxidize and precipitate as MnO_2. However, the kinetics of this reaction are sufficiently slow that precipitation would probably not occur until after the water was pumped from the well. Hem (1985) report that iron oxidation occurs on the order of minutes, whereas manganese oxidation requires several hours to a day under commonly encountered ground-water conditions. Accordingly, given the same environment, iron will be oxidized more rapidly than manganese.

Table 17. Selected physical and chemical properties of water samples from the Valle de Yabucoa alluvial aquifer, Puerto Rico

[T, Temperature is in degrees Celsius; pH is in pH units; S.C., specific conductance in microsiemens per centimeter; D.O., dissolved oxygen in milligrams per liter; Alk., alkalinity in milligrams per liter; DOC, dissolved organic carbon in milligrams per liter; Eh, Eh in millivolts; all concentrations are in milligrams per liter; nd, not determined]

Well number	Local well names	Date	T	pH	S.C.	D.O.	Alk.	NO_3 as N	NO_2 plus NO_3 as N	PO_4 as P	DOC	HS	Eh
1	Sun Oil #01 Well	August 23, 1988	26.9	7.15	804	4.6	202	nd	0.28	0.06	0.6	0.5	nd
2	Sun Oil #02 Well	August 23, 1988	26.9	7.43	772	4.9	162	nd	0.1	0.05	0.6	0.5	nd
3	Sun Oil #03 Well	August 23, 1988	26.9	7.34	810	2.2	201	nd	0.1	0.05	0.5	2.7	nd
4	Sun Oil #04 Well	September 8, 1988	27.0	7.04	634	1.1	235	nd	0.1	0.07	0.8	7.8	nd
5	Sun Oil #06 Well	August 23, 1988	26.5	7.49	490	5.0	171	nd	0.1	0.08	0.7	4.3	nd
6	Sun Oil #08 Well	September 8, 1988	26.9	6.29	390	1.7	161	nd	0.1	0.34	1.8	8.8	nd
7	Union Carbide #1, Pozo Valle #07	August 25, 1988	26.3	7.52	412	4.1	148	nd	0.3	0.04	0.4	0.5	nd
8	Union Carbide #2, Pozo Valle #10	August 25, 1988	26.7	7.90	461	4.7	195	nd	0.16	0.03	0.9	0.5	nd
9	Union Carbide #3, Pozo Valle #13	September 1, 1988	26.4	8.15	350	1.1	161	nd	0.1	0.01	0.8	0.5	nd
10	Union Carbide #4, Pozo Valle #14	August 25, 1988	26.7	7.90	461	4.7	176	nd	0.1	0.03	0.6	0.5	nd
11	Union Carbide #5	September 2, 1988	28.3	6.95	525	nd	221	nd	0.1	0.30	2.3	3.0	nd
12	Union Carbide #6, Pozo Valle #11	August 25, 1988	26.5	7.78	504	4.6	184	nd	0.19	0.04	0.9	3.0	nd
13	Pozo Calabazas	August 29, 1988	27.4	6.96	310	5.1	121	0.004	0.22	0.09	1.1	0.5	nd
14	Central Roig, Pozo Yabucoa #21	August 29, 1988	26.4	6.91	651	5.3	169	0.003	0.42	0.06	1.2	0.5	nd
15	Pozo de la Grúa, (PRASA)	August 26, 1988	26.7	7.45	397	4.9	141	nd	0.23	0.08	0.9	0.5	nd
16	Limones (PRASA), Pozo Central Roig	August 26, 1988	26.8	7.07	410	5.4	140	nd	0.54	0.07	0.8	0.5	nd
17	Viejo Roig (PRASA)	August 24, 1988	26.8	6.93	474	5.0	164	nd	0.24	0.04	0.6	0.5	nd
18	Guayanés (PRASA), Pozo Yabucoa	August 26, 1988	27.4	7.56	779	5.6	182	nd	0.1	0.08	0.5	0.5	nd
19	Test Well #08, Number 1	August 30, 1988	26.7	6.41	351	0.9	131	0.015	0.21	0.01	3.0	0.5	nd
20	Pozo Barrio Limones	September 1, 1988	27.1	7.77	1857	0.9	39	nd	0.1	0.01	0.7	2.2	nd

Table 17. Selected physical and chemical properties of water samples from the Valle de Yabucoa alluvial aquifer, Puerto Rico

[T, Temperature is in degrees Celsius; pH is in pH units; S.C., specific conductance in microsiemens per centimeter; D.O., dissolved oxygen in milligrams per liter; Alk., alkalinity in milligrams per liter; DOC, dissolved organic carbon in milligrams per liter; Eh, Eh in millivolts; all concentrations are in milligrams per liter; nd, not determined]

Well number	Local well names	Date	T	pH	S.C.	D.O.	Alk.	NO_3 as N	NO_2 plus NO_3 as N	PO_4 as P	DOC	HS	Eh
21	R.J. Reynolds #02, Valle #24	September 1, 1988	28.1	6.63	396	3.3	134	nd	0.1	0.30	0.8	0.5	nd
22	R.J. Reynolds #03, Valle #25	September 1, 1988	27.7	6.73	438	6.0	162	nd	0.21	0.77	0.6	4.6	nd
23	AH #02	September 6, 1988	27.3	7.28	399	1.7	123	0.006	0.27	0.04	0.5	5.9	nd
24	AH #03	September 6, 1988	26.2	6.99	454	1.2	176	0.008	0.1	0.02	0.4	0.5	nd
25	Pozo Martorell	September 6, 1988	26.7	6.29	431	1.0	135	0.006	0.1	0.02	1.3	0.5	nd
26	Manantial Rivera	September 7, 1988	24.5	7.07	164	7.6	48	nd	0.93	0.02	0.5	0.5	nd
27	Manantial F. Rojas	September 7, 1988	25.1	6.26	256	5.2	75	nd	2.1	0.03	0.7	9.6	nd
28	Manantial Rodríguez	September 7, 1988	26.5	6.65	384	6.0	138	nd	1.0	0.04	0.9	nd	nd
32	Playita 1	January 12, 1990	26.0	6.62	247	1.0	75	nd	1.3	0.04	1.9	nd	nd
32	Playita 1	April 4, 1990	27.6	7.60	520	2.2	238	0.021	0.4	0.06	4.8	nd	378
33	Playita 2	April 4, 1990	25.9	6.54	265	0.3	83	0.001	2.0	0.05	0.5	nd	116
34	Martorell 1	Mar. 28, 1990	27.0	6.33	175	0.2	nd	0.015	0.1	0.01	0.7	nd	48
34	Martorell 1	August 21, 1990	26.2	6.26	172	0.02	67	0.005	nd	nd	0.8	nd	82
35	Martorell 2	March 28, 1990	27.0	6.52	242	0.3	nd	0.013	0.1	0.01	0.7	nd	88
35	Martorell 2	August 21, 1990	26.2	6.51	235	0.02	98	0.009	0.1	0.07	0.6	nd	88
36	Limones 1	April 2, 1990	26.3	6.98	490	2.1	101	0.021	1.5	0.07	1.0	nd	439
37	Limones 2	April 2, 1990	26.4	6.64	310	0.1	130	0.019	0.1	0.01	1.1	nd	27
39	Juan Martín 1	March 29, 1990	26.0	7.17	625	0.0	129	0.028	0.4	0.04	0.5	nd	206
39	Juan Martín 1	August 23, 1990	26.7	7.11	640	0.04	123	0.005	0.4	0.03	0.4	nd	88
40	Juan Martín 2	March 29, 1990	26.3	6.98	510	2.1	128	0.031	0.1	0.04	0.4	nd	391
40	Juan Martín 2	August 23, 1990	26.5	6.93	560	0.02	124	0.005	0.1	0.03	0.6	nd	110
41	Juan Martín 3	March 29, 1990	27.0	6.22	339	0.0	106	0.013	0.1	0.01	1.6	nd	46
41	Juan Martín 3	August 23, 1990	26.7	6.22	338	0.08	114	0.005	0.1	0.03	1.7	nd	51
43	Sun 2	August 20, 1990	26.5	7.08	600	0.02	127	0.004	nd	nd	0.6	nd	-20
45	Harbor 2	August 22, 1990	27.1	7.34	875	0.06	335	0.002	0.1	0.04	2.3	nd	-39
46	Harbor 3	August 22, 1990	26.5	7.40	620	0.06	140	0.002	0.1	0.08	0.6	nd	42

Table 17. Selected physical and chemical properties of water samples from the Valle de Yabucoa alluvial aquifer, Puerto Rico--Continued

[T, Temperature is in degrees Celsius; pH is in pH units; S.C., specific conductance in microsiemens per centimeter; D.O., dissolved oxygen in milligrams per liter; Alk., alkalinity in milligrams per liter; DOC, dissolved organic carbon in milligrams per liter; Eh, Eh in millivolts; all concentrations are in milligrams per liter; nd, not determined]

Well number	Local well names	Date	Ca	Mg	Na	K	Cl	SO_4	F	SiO_2	Fe	Mn	Al
1	Sun Oil #01 Well	August 23, 1988	31	20	92	0.8	140	21	0.7	54	0.038	0.072	nd
2	Sun Oil #02 Well	August 23, 1988	40	19	81	1.3	130	26	0.6	54	0.009	0.220	nd
3	Sun Oil #03 Well	August 23, 1988	41	18	94	1.5	130	26	0.6	49	0.003	0.220	nd
4	Sun Oil #04 Well	September 8, 1988	40	16	58	1.2	55	6.8	0.6	56	0.330	0.440	nd
5	Sun Oil #06 Well	August 23, 1988	27	12	59	1.5	47	12	0.5	55	0.057	0.250	nd
6	Sun Oil #08 Well	September 8, 1988	25	12	29	1.7	25	5.8	0.3	54	9.400	0.760	nd
7	Union Carbide #1, Pozo Valle #07	August 25, 1988	28	13	38	1.9	31	13	0.3	49	0.032	0.046	nd
8	Union Carbide #2, Pozo Valle #10	August 25, 1988	31	17	49	2.4	39	15	0.4	51	0.009	0.094	nd
9	Union Carbide #3, Pozo Valle #13	September 1, 1988	26	13	54	1.9	51	16	0.4	38	2.900	0.099	nd
10	Union Carbide #4, Pozo Valle #14	August 25, 1988	30	16	43	2.0	33	11	0.4	48	0.008	0.120	nd
11	Union Carbide #5	September 2, 1988	40	16	36	2.5	24	10	0.3	50	10.000	1.000	nd
12	Union Carbide #6, Pozo Valle #11	August 25, 1988	32	16	47	2.2	40	16	0.4	49	0.012	0.230	nd
13	Pozo Calabazas	August 29, 1988	21	9.7	31	1.3	18	7.7	0.3	47	0.320	0.350	nd
14	Central Roig, Pozo Yabucoa #21	August 29, 1988	44	13	62	1.5	98	19	0.4	51	0.007	0.220	nd
15	Pozo de la Grúa, (PRASA)	August 26, 1988	23	11	46	1.9	34	9.1	0.4	53	0.086	0.075	nd
16	Limones (PRASA), Pozo Central Roig	August 26, 1988	20	10	51	1.2	44	8.5	0.4	60	0.010	0.016	nd
17	Viejo Roig (PRASA)	August 24, 1988	32	17	36	1.4	44	16	0.3	54	0.007	1.100	nd
18	Guayanés (PRASA), Pozo Yabucoa	August 26, 1988	28	13	110	2.4	130	32	0.7	51	0.023	0.220	nd
19	Test Well #08, Number 1	August 30, 1988	23	8.1	27	1.2	29	5.7	0.2	51	18.000	1.600	nd
20	Pozo Barrio Limones	September 1, 1988	120	13	220	2.5	500	140	0.3	21	0.062	0.100	nd

Table 17. Selected physical and chemical properties of water samples from the Valle de Yabucoa alluvial aquifer, Puerto Rico--Continued

[T, Temperature is in degrees Celsius; pH is in pH units; S.C., specific conductance in microsiemens per centimeter; D.O., dissolved oxygen in milligrams per liter; Alk., alkalinity in milligrams per liter; DOC, dissolved organic carbon in milligrams per liter; Eh, Eh in millivolts; all concentrations are in milligrams per liter; nd, not determined]

Well number	Local well names	Date	Ca	Mg	Na	K	Cl	SO$_4$	F	SiO$_2$	Fe	Mn	Al
21	R.J. Reynolds #02. Valle #24	September 1, 1988	23	9.7	45	1.5	30	15	0.2	42	0.820	3.600	nd
22	R.J. Reynolds #03. Valle #25	September 1, 1988	5.8	4.2	83	1.8	35	7.3	0.6	57	0.140	0.270	nd
23	AH #02	September 6, 1988	26	11	30	0.9	25	7.4	0.1	47	2.000	1.400	nd
24	AH #03	September 6, 1988	32	18	41	1.7	37	8.2	0.3	58	16.000	1.200	nd
25	Pozo Martorell	September 6, 1988	32	12	36	0.9	44	4.6	0.2	44	9.900	3.100	nd
26	Manantial Rivera	September 7, 1988	14	3.8	15	0.4	13	9.4	0.2	42	0.320	0.076	nd
27	Manantial F. Rojas	September 7, 1988	21	6.4	21	1.2	23	10	0.1	46	0.072	0.035	nd
28	Manantial Rodríguez	September 7, 1988	33	14	30	0.8	28	17	0.1	60	0.080	0.030	nd
32	Playita 1	January 12, 1990	17	5.7	22	1.3	19	11	0.1	36	0.011	0.22	nd
32	Playita 1	April 4, 1990	28	10	66	2.2	22	13	0.4	32	0.047	2.70	0.03
33	Playita 2	April 4, 1990	19	6.5	22	2.2	20	11	0.2	35	0.013	0.14	0.01
34	Martorell 1	March 28, 1990	7	2.6	11	0.7	7.8	10	0.2	45	19	0.48	0.01
34	Martorell 1	August 21, 1990	nd	nd	nd	nd	nd	nd	nd	nd	nd	nd	nd
35	Martorell 2	March 28, 1990	12	4.4	16	1.0	11	13	0.2	56	21	1.00	0.01
35	Martorell 2	August 21, 1990	12	4.2	15	1.0	11	13	0.4	50	22	1.00	0.01
36	Limones 1	April 2, 1990	17	7.4	67	1.5	56	19	0.3	51	0.012	0.67	0.01
37	Limones 2	April 2, 1990	19	6.9	23	1.5	19	2.6	0.2	54	13	1.20	0.01
39	Juan Martín 1	March 29, 1990	20	8.3	88	2.0	95	23	0.4	51	0.024	1.50	0.01
39	Juan Martín 1	August 23, 1990	21	8.3	90	1.9	100	30	0.5	52	0.031	0.76	0.01
40	Juan Martín 2	March 29, 1990	19	8.8	69	2.2	71	11	0.3	56	0.014	0.08	0.01
40	Juan Martín 2	August 23, 1990	20	9.2	73	2.0	78	19	0.6	55	0.17	0.23	0.01
41	Juan Martín 3	March 29, 1990	19	6.7	19	2.5	31	29	0.1	39	28	0.97	0.01
41	Juan Martín 3	August 23, 1990	19	6.8	21	2.6	28	27	0.7	33	28	0.97	0.01
43	Sun 2	August 20, 1990	nd	nd	nd	nd	nd	nd	nd	nd	nd	nd	nd
45	Harbor 2	August 22, 1990	61	28	75	1.4	83	4.1	0.5	55	0.02	1.40	0.02
46	Harbor 3	August 22, 1990	26	11	76	1.4	88	18	0.5	53	0.018	1.40	0.02

Table 18. Values for Eh, pH, and iron and manganese concentrations for water samples collected from the Valle de Yabucoa, Puerto Rico and plotted in figure 8

Sample number in figure 8	Well name	Date	pH	Eh, in millivolts	Iron, in milligrams per liter	Manganese, in milligrams per liter
1	Playita 2	April 4, 1990	6.54	378	0.013	0.14
2	Martorell 1	March 28, 1990	6.33	116	19	0.48
3	Martorell 1	August 21, 1990	6.26	48	19	0.47
4	Martorell 2	March 28, 1990	6.52	82	21	1.00
5	Martorell 2	August 21, 1990	6.51	88	22	1.00
6	Limones 1	April 2, 1990	6.98	439	0.012	0.67
7	Limones 2	April 2, 1990	6.64	27	13	1.20
8	Juan Martín 1	March 29, 1990	7.17	206	0.024	1.50
9	Juan Martín 1	August 23, 1990	7.11	88	0.031	0.76
10	Juan Martín 2	March 29, 1990	6.98	391	0.014	0.081
11	Juan Martín 2	August 23, 1990	6.93	110	0.17	0.23
12	Juan Martín 3	March 29, 1990	6.22	46	28	0.97
13	Juan Martín 3	August 23, 1990	6.22	51	28	0.97
14	Harbor 2	August 22, 1990	7.34	-39	0.020	1.40
15	Harbor 3	August 22, 1990	7.40	42	0.018	1.40

A careful analysis of the data reveals that high-production industrial and public-supply wells yielded water with relatively low iron and manganese concentrations, whereas abandoned and small private wells producing relatively small amounts of water yielded water with higher iron and manganese concentrations. The histograms in figure 9 illustrate the distribution of iron and manganese within both data subsets. The data in figure 9 were logarithmically transformed, and the resulting distributions in each of the histograms are approximately normal in the case of the abandoned and small private wells. Because the data are lognormally distributed, the geometric mean is presented in table 19 to represent the best measure of central tendency.
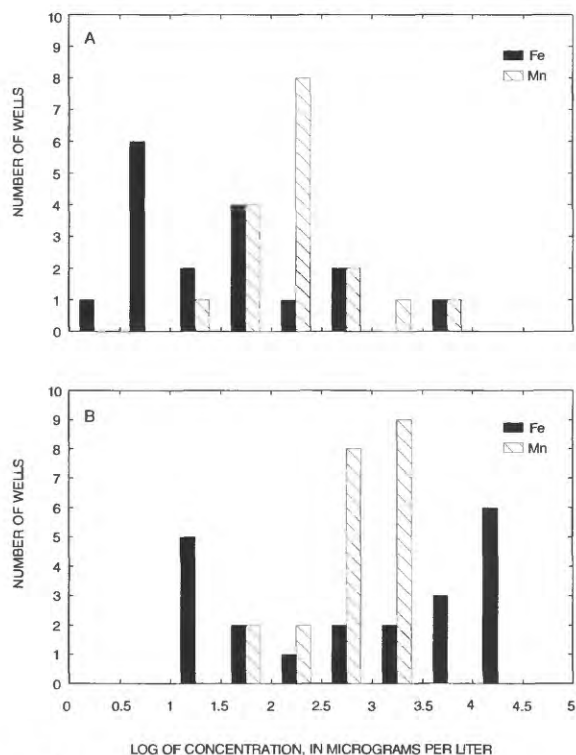
Figure 9. Distribution of iron and manganese concentrations in water pumped from (A) abandoned and small private wells and from (B) high-production industrial and public-supply wells.

The discrepancy in iron and manganese concentrations between the two types of wells indicate that well pumping characteristics can effect the magnitude of iron and manganese concentrations. The most likely explanation for this finding is that the wells producing large volumes of water are causing ground-water aeration in the vicinity of the pumping horizon. The aeration of ground water may result from the cascading of ground water inside well bores having two or more screened intervals or the rapid flow of ground water through the gravel pack surrounding the well bore. The aeration of ground water by one or more of these processes is thought to increase the redox potential in the immediate vicinity of the screened horizon to the point at which the oxidation of iron and, to a lesser degree, the oxidation of manganese can occur, resulting in the precipitation of the corresponding hydroxides in the aquifer, well, lift pipe, and distribution system.

The data in table 19 confirm the thermodynamic and kinetic expectations; for artificially oxygenated water (from large, continuous-production industrial and water-supply wells), the mean iron concentration is about 20 times lower than the mean iron concentration of un-oxygenated well water samples (from abandoned wells and wells with low production) whereas the mean manganese concentration of artificially oxygenated ground water samples was only about 3 times lower than in anoxic water samples.

Based on the findings discussed above, all iron and manganese concentrations measured in water samples collected from large industrial and water-supply wells are considered as nonrepresentative of actual, aquifer conditions. In addition, the March 1990 chemical analyses of water from the Martorell 1, Martorell 2, Juan Martín 1, Juan Martín 2, and Juan Martín 3 wells may also not represent actual aquifer conditions because the samples were taken only a few days after the wells had been developed with compressed air.

The distribution of iron and manganese, based on the chemical analyses of water from wells which do not appear to significantly oxygenate ground water, is depicted in figure 10 and figure 11. Low iron concentrations were measured near the boundary of the aquifer, where recharge occurs. Low iron concentrations were also measured in water from three shallow wells in the central portion of the aquifer, Limones 1, Juan Martín 1, and Juan Martín 2; however, at these sites the iron concentration increased greatly with depth. To better represent average aquifer conditions, the data from these shallow wells are not presented in figure 10, instead the data from the deep wells, Limones 2 and Juan Martín 3 are presented in figure 10.

The iron concentration in the ground water increases rapidly from the low concentrations observed near the boundaries of the aquifer and in shallow wells. After this rapid increase the concentrations then decrease near the center of the valley. Water from wells in the center of the valley with low iron concentrations frequently has a slight hydrogen sulfide odor. If hydrogen sulfide is present in the water, the iron has probably precipitated out of the ground water as an iron sulfide mineral.

Table 19. Geometric mean concentrations of iron and manganese in water produced from high-production industrial and municipal water-supply wells (high) and abandoned and low production private wells (low) in the Valle de Yabucoa, Puerto Rico

[mg/L, milligrams per liter]

| Production level	Iron concentration range (mg/L)	Geometric mean of iron concentration (mg/L)	Manganese concentration range (mg/L)	Geometric mean of manganese concentration (mg/L)
High	less than 0.003 to 10	0.038	0.02 to 3.6	0.207
Low	0.012 to 28	0.831	0.01 to 3.1	0.712
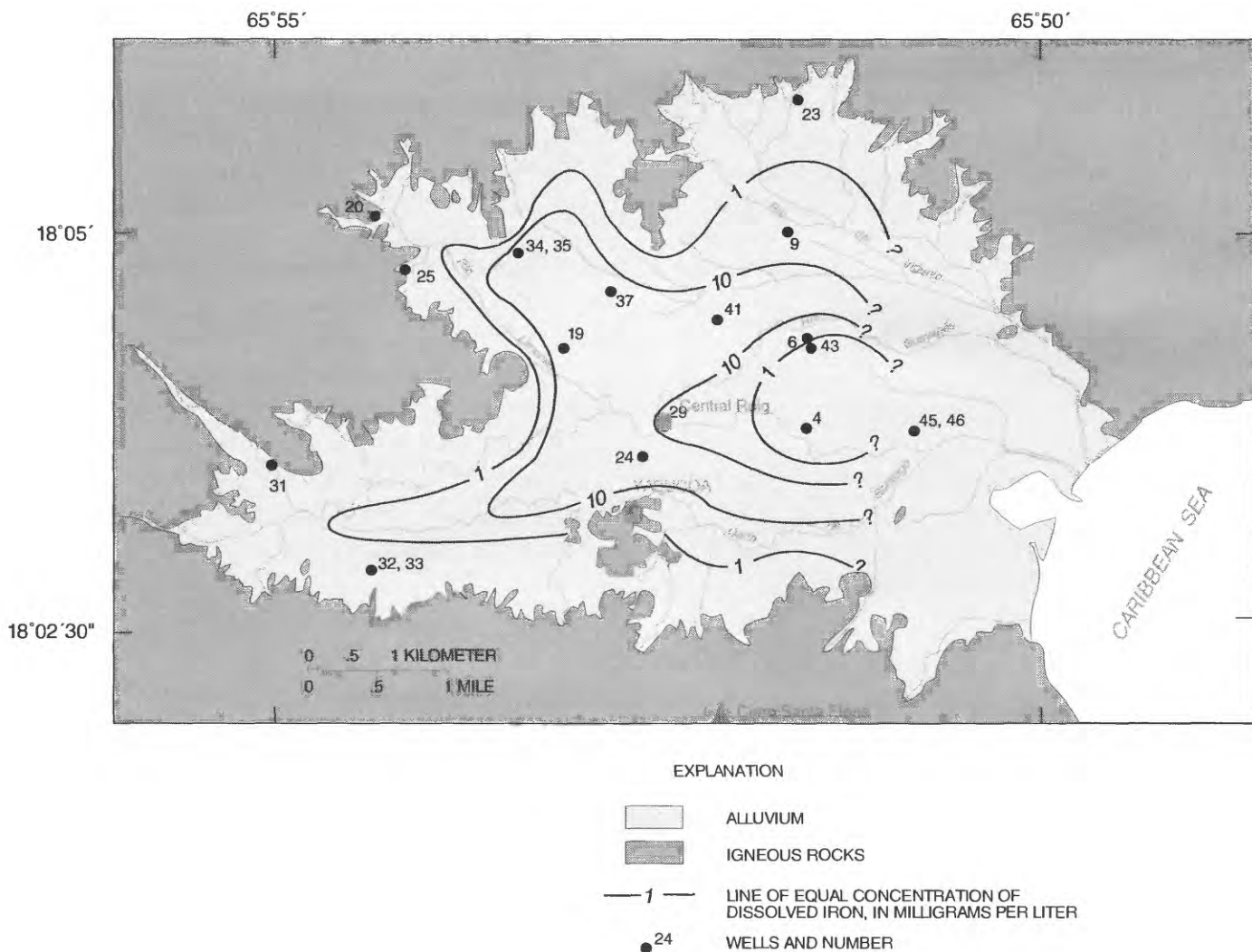
Figure 10. Distribution of iron in water in the Valle de Yabucoa alluvial aquifer, Puerto Rico.

The geographic distribution of manganese (fig. 11) is similar to that of iron. High manganese concentrations were measured in the center of the valley, and lower concentrations occurred in the recharge zone. The variation in manganese concentration is considerably less than the variation of iron concentration. Manganese concentrations are somewhat lower in the three down-gradient wells: Sun Oil #4 Well, Sun Oil #8, and Union Carbide #3 (numbers 4, 6, and 9 in table 3 and fig. 4).

The actual three-dimensional distribution of both iron and manganese is more complicated than indicated on figures 10 and 11. The observation wells at the Martorell, Limones, and Juan Martín well sites were carefully constructed to be open to only certain depths in the aquifer. The chemical analyses (table 18) clearly indicate that Eh decreases with depth, whereas iron and manganese increase with depth in the aquifer. Similar chemical changes with depth probably occur throughout the aquifer, but detailed information on these changes with depth is only available only for these three well sites.
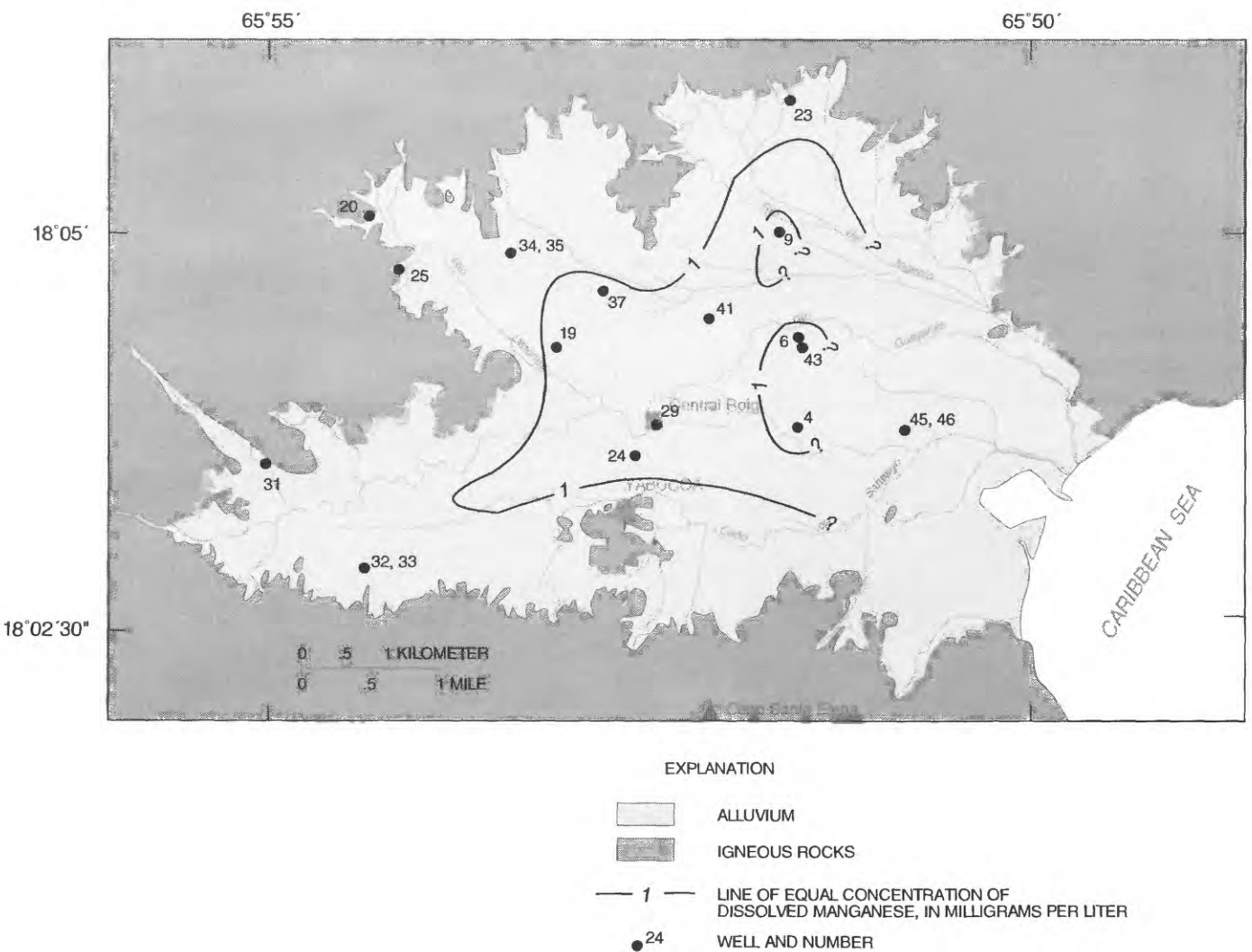
Figure 11. Distribution of manganese in water in the Valle de Yabucoa alluvial aquifer, Puerto Rico.

Sources and Sinks of Iron and Manganese

Electron and optical microscopy, energy dispersive spectroscopy, and x-ray diffraction have identified several iron-containing minerals that are weathering and releasing iron into the ground water. These minerals include plagioclase, calcian amphibole, biotite, magnetite, hematite, ilmenite, and iron oxide coatings on grains. Mechanisms of iron introduction into the ground water include both the dissolution of ferrous iron-bearing minerals and the reduction of ferric oxides. Reducing conditions [Eh ranges from +439 to -30 millivolts], in the majority of the aquifer maintain much of the ground water within the region of thermodynamic stability of the Fe^{2+} ion,

which enables the dissolution of iron from the iron bearing minerals in the aquifer. Loss of ferrous iron from these minerals is probably responsible for most of the observed elevated iron concentrations.

The largest contributor of ferrous iron to the ground water appears to be an iron oxide phase (probably maghemite, γ-Fe_2O_3, an alteration of magnetite). Petrographic observations indicate that maghemite has been removed leaving behind a skeleton of hematite on the (111) planes of the original magnetite crystal. This agrees with the saturations indexes calculated by the WATEQ4F water-quality computer model (Ball and Nordstrom, 1991). The results from WATEQ4F model indicates that the

reducing ground water in most of the aquifer is slightly under saturation with maghemite and oversaturated with both magnetite and hematite.

Only two mineral phases in the aquifer have been found to contain detectable manganese; amphibole and ilmenite. Trace amounts of manganese were found in the amphibole; however, the low concentrations and the fact that amphibole is not extensively corroded make it unlikely that this mineral is the primary source of the relatively high manganese concentrations found in the water. Ilmenite, $(Fe,Mn)TiO_3$, constitutes approximately 0.2 percent of the sediment, contains from 0 to 20 percent manganese substituting for iron in a solid solution with pyrophanite, $MnTiO_3$, and is probably the sole significant source of manganese. Individual ilmenite grains contain patches and streaks of leucoxene (a combination of rutile, TiO_2; anatase, TiO_2; and sphene, $CaTiO(SiO_4)$), indicating that leaching of iron and manganese from the original ilmenite has resulted in the formation of the iron and manganese-free alteration product and the release of the manganous and ferrous ions into the reducing ground water without oxidation or reduction reactions. The liberation of iron and manganese during the progressive alteration of ilmenite to leucoxene (possibly including the intermediate alteration product pseudo-rutile) has been reported by other workers (Morad and Aldahan, 1985; Anand and Gilkes, 1984).

Only one authigenic mineral appears to be forming in the aquifer and serving as a sink for iron or manganese. Some iron is removed from the ground water by the precipitation of 2- to 5-mm euhedral crystals of chalcopyrite.

A mass-balance geochemical model was derived using methods described by Plummer and others (1983) with the aid of the NETPATH computer program (Plummer and others, 1991) to account for the chemical evolution of water in composition the aquifer. In the mass-balance model andesine, amphibole, ilmenite, and biotite dissolve; organic carbon is oxidized; dissolved carbon dioxide gas is supplied from an external source; calcium is exchanged for sodium; and silica, goethite, kaolinite, and chalcopyrite are precipitated. Results of geochemical mass-balance modeling of the water

chemistry agree with the optical and electron microscopy data (Troester and others, 1990a; b).

Saline Intrusion

As ground water flows through the Valle de Yabucoa alluvial aquifer to the sea, chemical reactions between the water and the aquifer slowly increase the dissolved solids in the water and change the chemical characteristics of the water. Specific conductance can be readily measured in the field, and dissolved-solids concentrations (in milligrams per liter) can be estimated by multiplying the specific conductance value (in microsiemens per centimeter) by 0.59. For example, 12,000 μS/cm is approximately equal to about 7,000 mg/L dissolved solids. For reference, typical ocean water has a dissolved-solids concentration of about 34,000 mg/L.

The specific conductance measurements of the water in the aquifer ranged from less than 200 μS/cm in a shallow well at the western edge of the aquifer (Martorell 1, table 17) to more than 12,000 μS/cm in the deep observation well (table 14). Prior to drilling the deep observation well, the maximum measured specific conductance of water in the aquifer was 875 μS/cm (at the Harbor 2 well; table 17), and the measurements averaged about 500 μS/cm. Ground water with a specific conductance value of 875 μS/cm typically will have a dissolved solids concentration near the U.S. Environmental Protection Agency secondary drinking water standard for total dissolved solids of 500 mg/L (U.S. House of Representatives, 1996).

All of the complete chemical analyses in table 17 are plotted in figure 12, with the exception of the three springs (numbers 25 to 28) and Pozo Barrio Limones (number 20). The ground-water chemistry of the three springs is not representative of the Valle de Yabucoa alluvial aquifer because the springs issue from the igneous rocks that surround the Valle de Yabucoa. In addition the ground-water chemistry in the one sample from the Pozo Barrio Limones does not appear to reflect the chemistry of the aquifer, which may be because this private well was not properly developed prior to sampling.

The large arrows in figure 12 indicate the general trends in the chemistry of the aquifer. In the up-gradient portion of the aquifer the water is typically rich in calcium, magnesium, and bicarbonate. As the water moves through the aquifer and approaches the ocean, it becomes rich in sodium, potassium, and chloride. Additional details on the interpretation of Piper diagrams can be found in Piper (1944; 1953) and Briel (1993).

Unfortunately, little time series data exist that indicate the changes in ground-water chemistry that occur as a well is effected by saline intrusion. Usually, shortly after a well has been affected the well is abandoned and, subsequently, destroyed. For example, when water from the Sun Oil #1 well (the closest industrial supply well to the ocean) was sampled, the water had one of the highest specific conductance values measured, and the well has since been taken out of service and destroyed.

EXPLANATION

GENERAL TREND IN GROUND-WATER CHEMISTRY
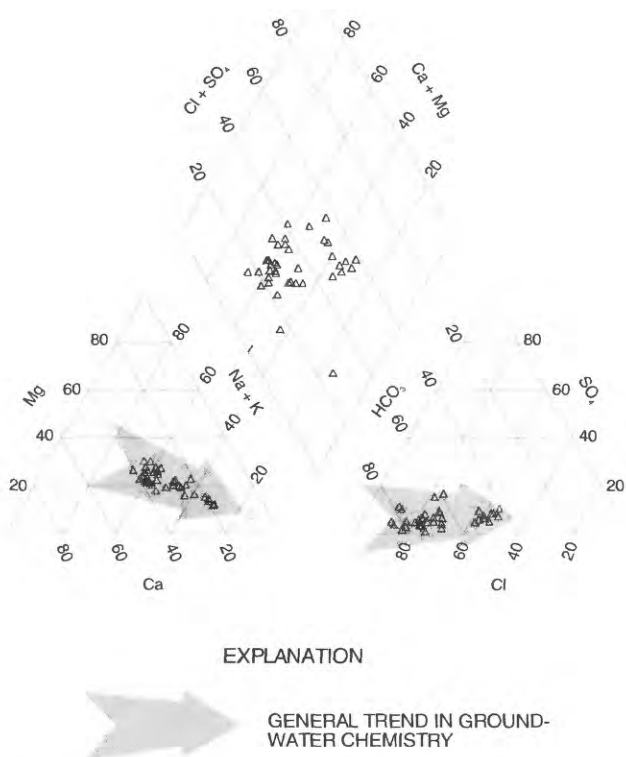
Figure 12. Piper diagram showing overall composition of sampled water in the Valle de Yabucoa alluvial aquifer, Puerto Rico.

Continued monitoring of the deep observation well may document changes in the ground-water chemistry at that site; however, the values that are listed in table 14 are approximately within the error in measuring specific conductance.

RESULTS OF THE GEOPHYSICAL SURVEY

Geophysical data were obtained at 84 sites in the Valle de Yabucoa using the TC method and at 31 sites using the TEM method. Six sets of the 84 data sets produced using the TC method were not used in this study because of interpretation problems believed to be caused by the nearby presence of scrap metal.

The apparent conductivity data produced from the TC method were analyzed and are presented in two different ways. First, some of the actual field measurements of apparent conductivity were plotted on a map of the area and contoured. Later each individual set of apparent conductivity measurements was modeled with a computer program to determine the depth to bedrock at each site. These depth-to-bedrock data were then combined with other depth-to-bedrock data to produce a map of the altitude of the top of the bedrock surface beneath the aquifer.

The contour map produced from the data obtained with the 40-m coil separation in the horizontal dipole (H40) orientation is shown in figure 13. The map is based on 78 data points. With this coil separation and orientation, 50 percent of the signal received is from less than upper 16 m depth and 80 percent of the signal received is from less than 40 m depth.

As expected, the apparent conductivity of the ground is highest near the coast. Readings of 100 mS/m or more are found only near the coast. The shape of both the 200 mS/m and the 100 mS/m contours are generally similar to the coastline; however, both contours are farther from the coast north of the harbor, than they are south of the harbor.

There is a large lobe of medium (75-100 mS/m) apparent conductivity extending inland north of the Caño de Santiago. This lobe of medium apparent conductivity is interpreted to be a paleochannel that

was cut through the ridge of bedrock when sea levels were as much as 120 m lower than today during the last glacial maximum (Fairbanks, 1989). The medium values of apparent conductivity in this area probably represent saline water near the base of the Valle de Yabucoa alluvial aquifer. Thus the specific conductance of this water should be equal to or greater than the specific conductance of the water at the deep observation well, which averages about 12,000 µS/cm.

The lobe of medium apparent conductivity separates two areas of low (less than 50 mS/m) apparent conductivity, one large area west of the harbor and another smaller area north of the harbor. The area of low apparent conductivity west of the harbor corresponds to the buried Harbor Ridge discussed by Anders (1971) and shown on figure 1. The area of low apparent conductivity north of the harbor is probably another buried ridge in the bedrock topography. This second ridge was not recognized by Anders (1971) because he lacked data from this small area.

EXPLANATION

IGNEOUS ROCKS

—50— LINE OF EQUAL TERRAIN CONDUCTIVITY, in mS/m

■ TERRAIN CONDUCTIVITY SITE
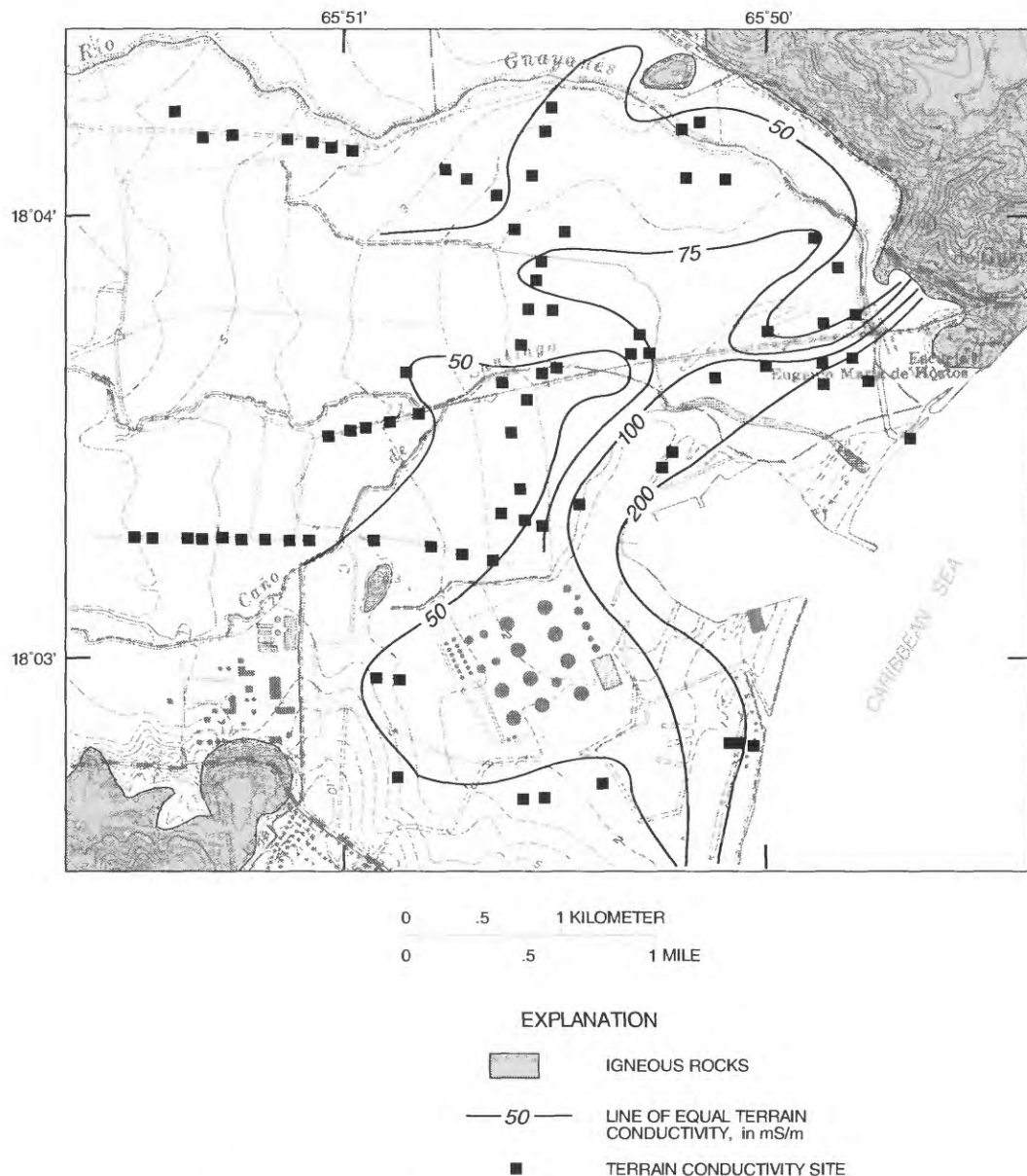
Figure 13. Apparent conductivity data from TC method using a 40-m coil separation and a horizontal dipole (H40) in the Valle de Yabucoa, Puerto Rico.

The high values (more than 100 mS/m) of apparent conductivity near the coast probably are caused by saline water in the alluvium east of the two buried ridges. North of the harbor, the steep gradient of apparent conductivity values indicates that the saline water ends abruptly where it abuts the bedrock ridge.

A second method of presenting the data from the TC method required the construction of geoelectric models that best fit each set of apparent conductivity measurements. This is accomplished with the EMIX34 computer program by Interpex. This program requires the operator to select an initial geoelectric model, which includes the number of layers and the thickness and connectivity of each layer. The computer program then determines the geoelectric model that best fits the apparent conductivity data by the method of inversion. The initial selection of layers and corresponding conductivities is based on knowledge of the geology of the site and an examination of the apparent conductivity data. In most cases, a number of different initial models were tried. In areas where the geology appeared to be laterally homogenous, the final model at one site was used as the starting model for adjacent sites.

For the 84 sets of data produced with the TC method, a 2-layer model was used at 44 sites, a 3-layer model at 28 sites, and at 12 sites it was not possible to find a model that fit the data well. At 6 of the 12 sites that were not modelled the apparent conductivity was above 100 mS/m.
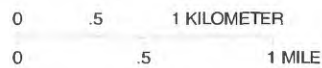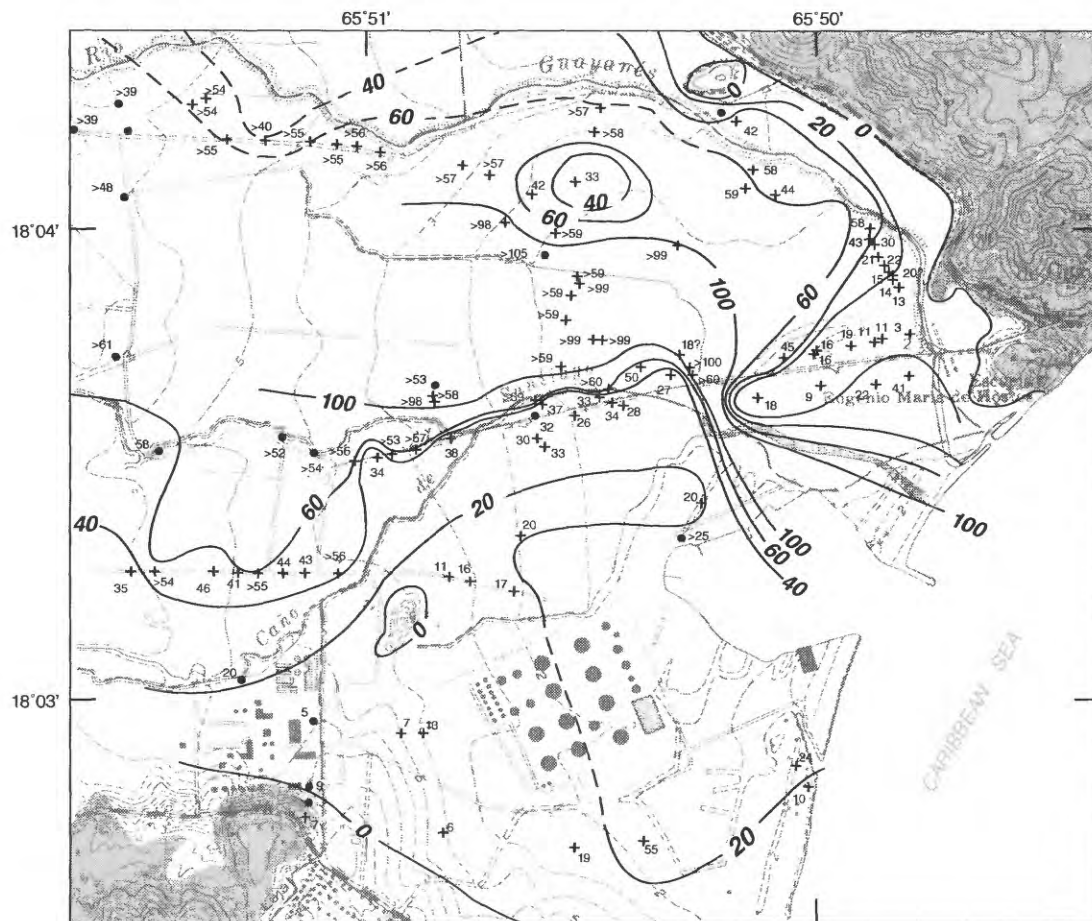
A similar procedure was used with the 31 data sets produced with the TEM method. These sites were modeled with the TEMIX47 computer program by Interpex.

The geoelectric models of the geophysical data were then interpreted based on the geologic knowledge of the valley and the available driller's log data. Conductivity ranged from 5 to 200 mS/m for unsaturated alluvium and alluvium saturated with freshwater and from 100 to 300 mS/m for alluvium saturated with saline water. The conductivity of the bedrock in the area, generally was less than 10 mS/m. In parts of the study area, it was difficult distinguishing between clayey alluvium saturated with freshwater and alluvium saturated with brackish water on the basis of conductivity measurements.
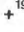
The interpretation of the geoelectric models produced form the data obtained with both the TC and TEM methods and the available data from wells drilled in the lower part of the Valle de Yabucoa were used to produce a map of the altitude of the top of the bedrock underlying the aquifer (fig. 14). This map is similar to the map of altitude of the top of bedrock produce by Robison and Anders (1973, p.4), which is reproduced in this report as figure 15.

The two maps are similar, but figure 14 does provide more detailed information in the crucial area near the coast. Figure 14 clearly shows a paleochannel incised in the bedrock just north of and roughly parallel to the Caño de Santiago. This paleochannel forms a narrow canyon that separates the Harbor Ridge from the buried bedrock ridge which extends from the northern side of the valley. The map indicates that in a space of less than 600 m, the bedrock-alluvium contact decreases from 50 m below sea level to more than 100 m below sea level and then increases to 45 m below sea level. Further inland the channel widens out. The deep observation well was drilled into the wider portion of this paleochannel.
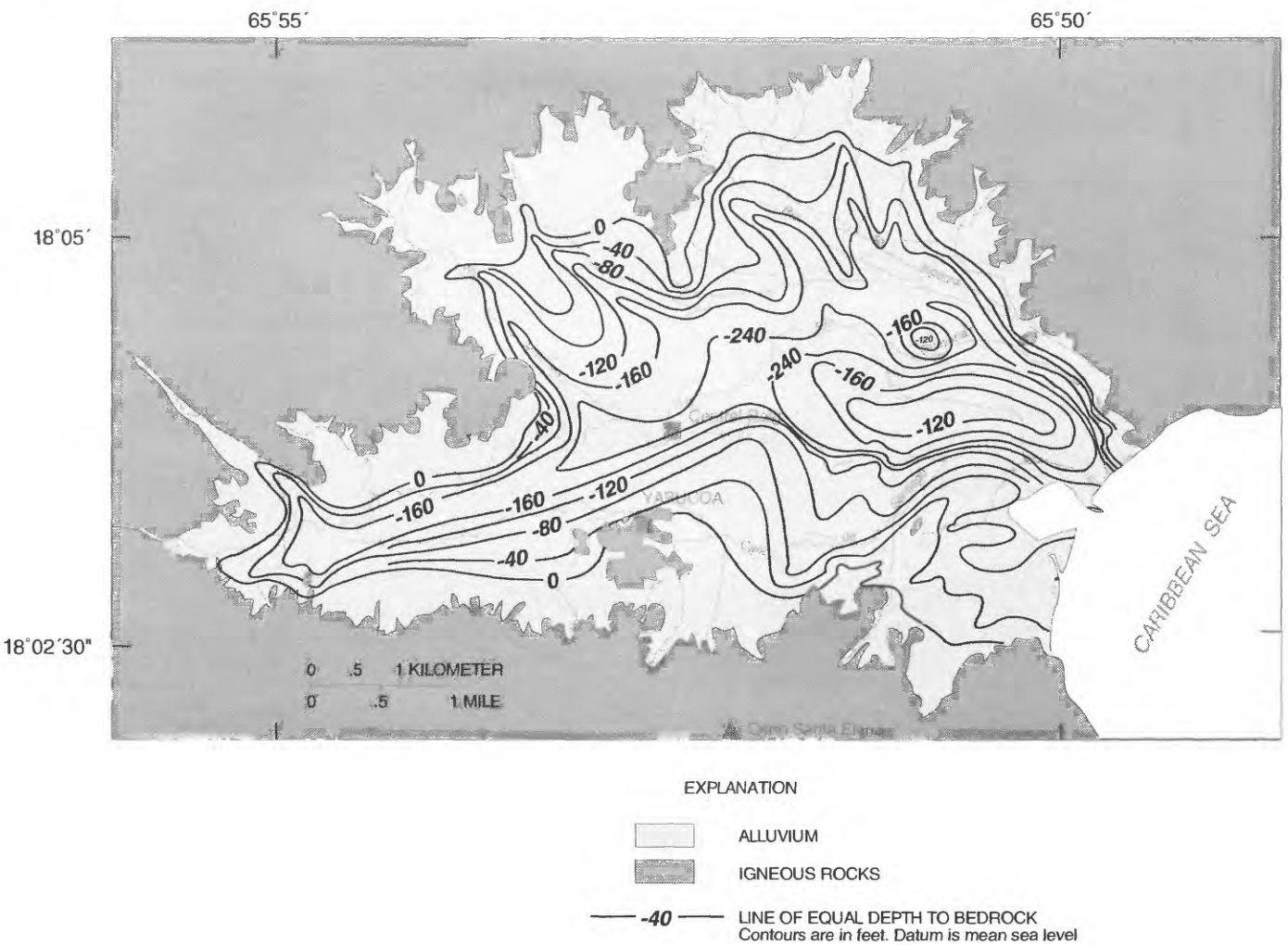
Figure 14. Map of the altitude of the top of bedrock in the Valle de Yabucoa, Puerto Rico (map is based on well data and surface geophysical measurements.

Figure 15. Map of the elevation of the top of bedrock in the Valle de Yabucoa, Puerto Rico (from Robison and Anders, 1973, p. 4) based on the drilling data available in 1970. Contours are in feet below mean sea level.

SUMMARY

The Valle de Yabucoa alluvial aquifer, in southeastern Puerto Rico, is the municipal and industrial water supply for the town of Yabucoa. The aquifer consists of more than 100 m of alluvium overlying relatively impermeable bedrock. Water samples collected from the aquifer have iron and manganese concentrations as high as 28 and 3.6 mg/L, respectively. Although the elevated iron and manganese concentrations in the aquifer pose no health threat, they frequently exceed the secondary standards for drinking water. In addition, dissolved solids concentrations in some shallow ground-water samples approach the 500-mg/L secondary drinking water standard for total dissolved solids.

Pumping from the aquifer for industrial use and public supply has lowered the water table to below sea level in some areas and has reversed the natural gradient of the water table towards the ocean. The saline-freshwater interface appears to have migrated landward because of this gradient reversal. A subsequent reduction in pumping has caused the water table to rise and may have stopped the landward migration of saline water.

Two surface electromagnetic geophysical techniques (the terrain conductivity method and the transient electromagnetic method) were used to map depth to bedrock and to determine the position of the saline-freshwater interface. Pumping and the shape of the bedrock-alluvium contact appear to control the extent and location of the saline-freshwater interface. The data indicate that saline-water intrusion is probably confined to the deepest part of the aquifer in a narrow paleochannel incised in the bedrock.

REFERENCES

Anand, R.R., and Gilkes, R.J., 1984: Weathering of ilmenite in a lateritic pallid zone: Clays and Clay Minerals, v. 32, n. 5, p. 363-374.

Anders, R.B., 1971, Electrical analog model study of water in the Yabucoa valley, Puerto Rico--Phase 1, collecting preliminary data and assembling available data: U.S. Geological Survey Open-File Report, 47 p.

Ball, J.W., and Nordstrom, D.K., 1991, User's manual for WATEQ4F, with revised thermodynamic data base and test cases for calculation speciation of major, trace, and redox elements in natural waters: U.S. Geological Survey Open-File Report 91-193, 189 p.

Boccheciamp, R.A., 1977, Soil survey of the Humacao area of eastern Puerto Rico: U.S. Department of Agriculture, Soil Conservation Service, 103 p.

Briel, L.I., 1993, Documentation of a multiple-technique computer program for plotting major-ion composition of natural waters: U.S. Geological Survey Open-File Report 93-74, 88 p.

Briggs, R.P., and Akers, J.P., 1965, Hydrogeologic map of Puerto Rico and adjacent islands: U.S. Geological Survey Hydrologic Investigation Atlas HA-197.

Cadilla, J.F., 1963, Geology of the Humacao titaniferous iron deposit: Caribbean Journal of Science, v. 3, no. 4, p. 243-247.

Calvesbert, R.J., 1970, Climate of Puerto Rico and U.S. Virgin Islands, revised: U.S. Environmental Science Services Administration, Climatography of the United States 60-52, 29 p.

Collar, P.D., Troester, J.W., Deike, R.G., and Robinson, P.D., 1990, Iron and manganese in alluvial ground water, Yabucoa, Puerto Rico: 22nd Congress of the Interamerican Association of Sanitary and Environmental Engineering, AIDIS, San Juan, Puerto Rico, v. 1, p. 708-732.

Colony, R.J., and Meyerhoff, H.A., 1935, The magnetite deposit near Humacao, Puerto Rico: American Institute of Mining and Metallurgical Engineers Transactions v. 115, p. 247-272.

Cox, D.P., and Briggs, R.P., 1973, Metallogenic map of Puerto Rico: U.S. Geological Survey Miscellaneous Geological Investigation Map I-721.

Cox, D.P., Marvin, F.F., M'Gonigle, J.W., McIntyre, D.H., and Rogers, C.L., 1977, Potassium-argon geochronology of some metamorphic, igneous, and hydrothermal events in Puerto Rico and the Virgin Islands: U.S. Geological Survey Journal of Research, v. 5, no. 6, p. 689-703.

Fairbanks, R.G., 1989, A 17,000-year glacio-eustatic sea level record: influence of glacial melting rates on the Younger Dryas event and deep-ocean circulation: Nature, v. 342, p. 637-642.

Fettke, C.R., 1924a, Geology of the Humacao district, Porto Rico: New York Academy of Science, Scientific Study of Porto Rico and the Virgin Islands, v. 2, pt. 2, p. 117-197.

_____ 1924b, Magnetic deposits of eastern Porto Rico: American Institute of Mining and Metallurgical Engineers Transactions, v. 70, p. 1024-1042.

Fields, F.K., 1971, Floods in the Yabucoa area, Puerto Rico: U.S. Geological Survey Hydrologic Investigation Atlas HA-382.

Fishman, M.J., and Friedman, M.J., 1989, Methods for determination of inorganic substances in water and fluvial sediments, 3d ed.: Techniques of Water-Resources Investigations of the United States Geological Survey, Chapter A1; U.S. Geological Survey Open-File Report, 545 p.

Fitterman, D.V., and Stewart, M.T., 1986 Transient electromagnetic sounding for groundwater: Geophysics, v. 51, p. 995-1005.

Giusti, E.V., and López, M.A., 1967, Climate and streamflow of Puerto Rico: Caribbean Journal of Science, v. 7, p. 87-93.

Guillou, R.B., and Glass, J.J., 1957, A reconnaissance study of the beach sands of Puerto Rico: U.S. Geological Survey Bulletin 1042-I, p. 273-305.

Hem, J.D., 1985: Study and interpretation of the chemical characteristics of natural water (3d ed.): U.S. Geological Survey Water-Supply Paper 2254, 264 p.

Lobeck, A.K., 1922, The physiography of Porto Rico: New York Academy of Science, Scientific Survey of Porto Rico and the Virgin Islands, v. 1, pt. 4, p. 301-379.

Marsh, S.P., 1992a, Analytical results for stream sediment and soil samples from the Commonwealth of Puerto Rico, Isla de Culebra, and Isla de Vieques: U.S. Geological Survey Open-File Report 92-353A, 8 p.

_____ 1992b, Analytical results for stream sediment and soil samples from the Commonwealth of Puerto Rico, Isla de Culebra, and Isla de Vieques: U.S. Geological Survey Open-File Report 92-353B, 5.25-inch diskette.

McNeill, J.D., 1980, Electromagnetic terrain conductivity measurement at low induction numbers: Geonics Limited, 15 p.

_____ 1983, EM34-3 survey interpretation techniques: Geonics Limited, 16 p.

_____ 1991, Use of electromagnetic methods for groundwater studies: Geotechnical and Environmental Geophysics: v. 2, p. 191-217.

Meyerhoff, H.A., 1933, Geology of Puerto Rico: Puerto Rico University Monograph, series B, no. 1, 306 p.

M'Gonigle, J.W., 1978, Geologic map of the Humacao quadrangle, Puerto Rico: U.S. Geological Survey Miscellaneous Investigation Map I-1070.

Morad, S., and Aldahan, A.A., 1985: Leucoxene-calcite-quartz aggregates in sandstones and the relation to decomposition of sphene: Neues J. für Mineralogie, v. 10, p. 458-468.

Piper, A.M., 1944, A graphic procedure in the geochemical interpretation of water analyses: American geophysical Union Transactions, v. 25, p. 914-923.

_____ 1953, A graphic procedure in the geochemical interpretation of water analyses [revised]: U.S. Geological Survey Ground Water Notes, Geochemistry, no. 12, 14 p.

Plummer, L.N., Parkhurst, D.L., and Thorstenson, D.C., 1983, Development of reaction model for ground-water systems: Geochimica et Cosmochimica Acta, v. 47, p. 665-686.

Plummer, L.N., Prestemon, E.C., and Parkhurst, D.L., 1991, An interactive code (NETPATH) for modeling net geochemical reactions along a flow path: U.S. Geological Survey Water-Resources Investigations Report 91-4078, 227 p.

Richards, R.T., and Troester, J.W., 1991, Mapping the saline-freshwater interface and the depth to bedrock in the Valle de Yabucoa alluvial aquifer with surface geophysical techniques: Abstracts and Program for the 17th Symposium of Natural Resources, San Juan, Puerto Rico, November 1991, p. 18-19.

Richards, R.T., and Troester, J.W., 1993, The use of surface geophysics to determine the best location for an observation well to monitor saline-water intrusion the Valle de Yabucoa alluvial aquifer, southeastern Puerto Rico: Advances in Water Resources Research in Puerto Rico and the U.S. Virgin Islands, San Juan, Puerto Rico, p. 38-39.

Robison, T.M., and Anders, R.B., 1973, Electrical analog model study of the alluvial aquifer in the Yabucoa valley, Puerto Rico--Phase 2, The planning, construction, and use of the model: U.S. Geological Survey Open-File Report 73-1, 22 p.

Rogers, C.L., 1977, Geologic map of the Punta Guayanés quadrangle, southeastern Puerto Rico: U.S. Geological Survey Miscellaneous Investigations Series Map I-998.

Rogers, C.L., Cram, C.M., Pease, M.H., Jr., and Tischler, M.S., 1979, Geologic map of the Yabucoa and Punta Tuna quadrangles, Puerto Rico: U.S. Geological Survey Miscellaneous Investigations Series Map I-1086, scale 1:20,000.

Troester, J.W., Collar, P.D., Robinson, P.D., and Deike, R.G., 1990a, Geochemical processes controlling manganese and iron concentrations in the ground water of the Valle de Yabucoa alluvial aquifer, Puerto Rico: EOS, Transactions, American Geophysical Union, v. 71, p. 506.

Troester, J.W., Deike, R.G., Robinson, P.D., and Collar, P.D., 1990b, Petrographic analyses and geochemical modeling of aqueous/solid phase reactions in the Valle de Yabucoa alluvial aquifer, Puerto Rico: Geological Society of America Annual Abstracts and Program, v. 22, no. 7, p. 295.

U.S. House of Representatives, 1996, Secondary maximum contaminant levels: Code of Federal Regulations, Title 40, Chapter I, Subchapter C, Part 143.

U.S. Geological Survey, 1994-96, Water resources data, Puerto Rico and the U.S. Virgin Islands, Water Years 1993-95: U.S. Geological Survey Water-Data Reports PR-93-1 to PR-95-1 (published annually).

Viessman, W., Jr., and Hammer, M.J., 1985: Water supply and pollution control (4th ed.): Harper & Row, 797 p.

Wood, W.W., 1976: Guidelines for collection and field analysis of ground-water samples for selected unstable constituents: Techniques of Water-Resources Investigations of the United States Geological Survey, Book 1, Chapter D2; 24 p.